Åbo Akademi

OPEN ACCESS

This is an electronic reprint of the original article. This reprint may differ from the original in pagination and typographic detail.

Stress-induced transcriptional memory accelerates promoter-proximal pause release and decelerates termination over mitotic divisions

Vihervaara, Anniina; Mahat, Dig Bijay; Himanen, Samu V.; Blom, Malin A.H.; Lis, John T.; Sistonen, Lea

Published in:
Molecular Cell

DOI:
10.1016/j.molcel.2021.03.007
10.1016/j.molcel.2021.03.007

Published: 15/04/2021

Document Version
Accepted author manuscript

Document License
CC BY-NC-ND

Link to publication

Please cite the original version:
Vihervaara, A., Mahat, D. B., Himanen, S. V., Blom, M. A. H., Lis, J. T., & Sistonen, L. (2021). Stress-induced transcriptional memory accelerates promoter-proximal pause release and decelerates termination over mitotic divisions. *Molecular Cell*, *81*(8), 1715-1731.e6. https://doi.org/10.1016/j.molcel.2021.03.007, https://doi.org/10.1016/j.molcel.2021.03.007

General rights
Copyright and moral rights for the publications made accessible in the public portal are retained by the authors and/or other copyright owners and it is a condition of accessing publications that users recognise and abide by the legal requirements associated with these rights.

Take down policy
If you believe that this document breaches copyright please contact us providing details, and we will remove access to the work immediately and investigate your claim.

This document is downloaded from the Research Information Portal of ÅAU: 11. May. 2024

Stress-Induced Transcriptional Memory Accelerates Promoter-Proximal Pause-Release and Decelerates Termination over Mitotic Divisions

Anniina Vihervaara[1,2,3,4]*, Dig Bijay Mahat[3,5,§], Samu V. Himanen[1,2,§], Malin A.H. Blom[1,2], John T. Lis[3]*, and Lea Sistonen[1,2]*¥

1) Faculty of Science and Engineering, Cell Biology, Åbo Akademi University, 20520 Turku, Finland.
2) Turku Bioscience Centre, University of Turku and Åbo Akademi University, 20520 Turku, Finland.
3) Department of Molecular Biology and Genetics, Cornell University, Ithaca, NY 14853, USA.
4) KTH Royal Institute of Technology, Department of Gene Technology, Science for Life Laboratory, 17165, Stockholm, Sweden.
5) Current address: Massachusetts Institute of Technology, Cambridge, MA 02139, USA.

* Correspondence: viher@kth.se or jtl10@cornell.edu or lea.sistonen@abo.fi
§ Equal contribution
¥ Lead contact

Keywords: Acquired stress resistance, chromatin accessibility, enhancer transcription, gene-enhancer networks, nascent transcription program, Pol II pausing, progression of Pol II, recycling of Pol II, transcription termination.

Summary

Heat shock instantly reprograms transcription. Whether gene and enhancer transcription fully recover from stress, and whether stress establishes a memory by provoking transcription regulation that persists through mitosis, remained unknown. Here, we measured nascent transcription and chromatin accessibility in unconditioned cells and in the daughters of stress-exposed cells. Tracking transcription genome-wide at nucleotide-resolution revealed that cells precisely restore RNA Polymerase II (Pol II) distribution at gene bodies and enhancers upon recovery from stress. However, a single heat exposure in embryonic fibroblasts primed a faster gene-induction in their daughter cells by increasing promoter-proximal Pol II pausing, and by accelerating the pause-release. In the daughters of repeatedly stressed cancer cells, both basal and heat-induced transcription was refined, and termination-coupled pre-mRNA processing decelerated. The slower termination retained transcripts on the chromatin and reduced recycling of Pol II. These results demonstrate that heat-induced transcriptional memory acts through promoter-proximal pause-release and pre-mRNA-processing at transcription termination.

Highlights

- Cell type-specific transcription precisely recovers after heat-induced reprogramming
- Heat induction of quality control genes is accelerated in the daughters of stressed cells
- Multiple heat shocks in cancer cells refine basal and inducible transcription over mitotic divisions
- Promoter-proximal Pol II pausing, pause-release and transcription termination are the rate-limiting steps involved in establishing a transcriptional memory
- Accessible chromatin spreads with heat-induced transcription to genes and enhancers
- HSF1 triggers promoter-proximal Pol II pause-release *via* distal and proximal regulatory elements

Introduction

Heat shock fires transcription reprogramming, provoking an instant genome-wide change in RNA synthesis from genes and enhancers (reviewed in Vihervaara *et al*., 2018). Upon heat shock, hundreds of genes are rapidly induced by a potent *trans*-activator heat shock factor 1 (HSF1). Activated HSF1 binds to heat shock elements (HSEs) at architecturally primed promoters and enhancers (Rougvie and Lis, 1988; Rasmussen and Lis, 1993; Guertin and Lis, 2010; Vihervaara *et al*., 2013; 2017; Ray *et al*., 2019), and it can trigger the release of promoter-proximally paused Pol II into productive elongation (Duarte *et al*., 2016; Mahat *et al*., 2016). Concomitantly with the heat-induced escape of Pol II from the promoters of activated genes, thousands of genes are repressed *via* inhibition of the Pol II pause-release. This restricted entry of Pol II into productive elongation causes the transcription machinery to accumulate at promoter-proximal regions of heat-repressed genes (Mahat *et al*., 2016; Vihervaara *et al*., 2017). As a consequence of the genome-wide re-coordination of Pol II pause-release, heat-stressed cells promptly switch their transcription program to produce chaperones, reduce genome-wide transcription, and protect cellular integrity.

Stress responses are robustly activated and evolutionarily conserved to safeguard cells and organisms. Severe stress can have long-lasting consequences for an individual (Guan *et al*., 2002; Sailaja *et al*., 2012) and cause physiological changes over generations (Kaati *et al*., 2002; Wei *et al*., 2014; reviewed in Heard and Martienssen, 2014). The inheritance of physiological changes to many types of stresses has been described, but the cellular mechanisms that establish, maintain and execute transcriptional memory remain poorly understood (reviewed in Perez and Lehner, 2019). Various stresses have been associated with long-term changes in the chromatin state (Guan *et al*., 2002; Tetievsky and Horowitch, 2010; Sailaja *et al*., 2012; D'Urso *et al*., 2016; Lämke *et al*., 2016; reviewed in D'Urso and Brickner, 2017), and shown to protect against protein misfolding by increasing chaperone expression (Gerner and Schneider, 1975; Maytin *et al*., 1990; Yost and Lindquist, 1991). However, stress-induced long-term changes in gene expression have been investigated with steady-state RNA and protein analyses, which neither capture the processes of nascent transcription nor reveal the mechanistic control of Pol II. Thus, we do not yet know whether cells restore or adjust their program of nascent RNA synthesis when recovering from stress, and whether regulation of Pol II at genes and enhancers encodes a memory of encountered stress.

Here, we provoked a genome-wide change in gene and enhancer transcription using heat shock and

82 asked whether proteotoxic stress reprograms transcription and transcriptional responsiveness over
83 mitotic divisions. We monitored nascent RNA synthesis at nucleotide resolution using Precision
84 Run-On sequencing (PRO-seq) that provides genome-wide maps of transcription-engaged Pol II
85 complexes at genes and enhancers (Kwak *et al*., 2013; Core *et al*., 2014; Vihervaara *et al*., 2017).
86 By tracking engaged Pol II complexes through the rate-limiting steps of transcription, PRO-seq
87 allows identification of regulatory decisions at high fidelity and spatiotemporal resolution
88 (reviewed in Cardiello *et al*., 2019; Wissink *et al*., 2019). Simultaneously, changes in the chromatin
89 accessibility were measured with an assay for transposase-accessible chromatin using sequencing
90 (ATAC-seq; Buenrostro *et al*., 2013). We used mouse embryonic fibroblasts (MEFs) and human
91 K562 erythroleukemia cells that coordinate transcription upon heat shock with similar mechanisms
92 (Mahat *et al*., 2016; Vihervaara *et al*., 2017), yet display different cellular identities, patho-
93 physiological states, and stress sensitivities (Lozzio and Lozzio, 1975; Mivechi 1989; Ahn *et al*.,
94 2001; Luft *et al*., 2001; Vihervaara *et al*., 2013; Elsing *et al*., 2014).
95
96 We found that transcriptional reprogramming by heat shock is followed by a precise restoration of
97 basal cell type-specific transcription program within hours of recovery. In accordance, chromatin
98 accessibility spread with transcription to heat-induced genes and enhancers and returned to pre-
99 stress levels during the recovery. This transient transcriptional response to stress enabled us to
100 investigate whether stress exposure establishes a transcriptional memory. In non-transformed
101 MEFs, a single heat shock primed a subset of genes for an instant induction in the daughter cells.
102 The faster responsiveness was established by increased promoter-proximal Pol II pausing and
103 accelerated pause-release upon an additional heat shock. In human K562 erythroleukemia cells,
104 repeated stress exposures decreased transcription of genes for protein synthesis and increased
105 transcription of pro-survival genes over mitotic division. The daughters of repeatedly heat-stressed
106 cells also prolonged the residency of Pol II at the termination window of active genes, concurrently
107 reducing transcript cleavage and recycling of Pol II to a new heat-induced initiation. These results
108 uncovered promoter-proximal Pol II pausing, pause-release and transcription termination as the
109 rate-limiting steps of transcription involved in establishing a memory over cell divisions.

110 **Results**

111

112 *Normalization of PRO-seq Data to Measure Rapid Transcription Kinetics and Prolonged*
113 *Transcription Changes*

114 We tracked the process of nascent transcription in acutely stressed cells, in cells recovering from
115 stress, and in the daughters of stress-exposed cells using PRO-seq. PRO-seq is a highly sensitive
116 method that maps engaged transcription complexes at nucleotide resolution across the genome
117 (Kwak *et al*., 2013), and provides instant measures of rate-limiting regulatory steps at genes and
118 enhancers upon transcriptional reprogramming (reviewed in Cardiello *et al*., 2019; Wissink *et al*.,
119 2019). Since heat shock causes a global change in nascent transcription (reviewed in Vihervaara *et*
120 *al*., 2018), robust normalization strategies are required to precisely quantify transcription between
121 distinct stress conditions. We normalized the PRO-seq datasets of short (<1-hour) heat shock (HS)
122 kinetics using ends of over 150 kb long genes, which provide sample-intrinsic normalization
123 windows beyond the reach of acute heat-induced changes in transcription (Mahat *et al*., 2016;
124 Vihervaara *et al*., 2017). For samples cultured more than an hour under distinct conditions, we
125 adopted a whole-genome spike-in strategy (Booth *et al*., 2018), and used *Drosophila* S2 cells as an
126 extrinsic source of PRO-seq normalization counts (see Materials and Methods). Accurate
127 normalization was evident from the highly similar Pol II densities at gene bodies between
128 biological replicate pairs (Figures S1 and S2), and close to identical transcription profiles of heat-
129 unresponsive genes, as demonstrated in cells cultured several days under distinct conditions
130 (Figures S1C and S2B).

131

132 *De Novo Identification of Transcribed Enhancers from Nascent Transcription Profile*

133 Active enhancers generally produce unstable and short enhancer RNAs (eRNAs) from divergent
134 initiation regions (Core *et al*., 2014; Henriques *et al*., 2018; Mikhaylichenko *et al*., 2018; Tippens
135 *et al*., 2018; Tome *et al*., 2018; Tippens *et al*., 2020). The specific pattern of eRNA transcription is
136 used for identification of transcribed enhancers *de novo* at high spatiotemporal resolution (Melgar
137 *et al*., 2011; Azofeifa and Dowell, 2017; Vihervaara *et al*., 2017; Chu *et al*., 2018; Wang *et al*.,
138 2019). There is no method for *in vivo* functional validation of all the computationally identified
139 enhancers, but we confirmed that the putative enhancers that we identified from PRO-seq
140 (dnasequence.org; Wang *et al*., 2019) precisely captured functionally verified enhancers of MYC
141 (Fulco *et al*., 2016) and beta globin locus control element (Li *et al*., 2002, Song *et al*., 2007) in
142 K562 cells (Figure S3A-B). The putative enhancers also contained the expected chromatin

143 modifications (Figure S3C), and 76% of them localized to transcription-associated chromatin loops
144 (Figure S3D). Our analyses strengthen and extend previous studies (Vihervaara *et al*., 2017;
145 Henriques *et al*., 2018; Mikhaylichenko *et al*., 2018; Chu *et al*., 2018; Wang *et al*., 2019; Tippens
146 *et al*., 2020), showing that promoter-distal transcription regulatory elements with divergently
147 oriented Pol II include functional enhancers. For simplicity, we refer to the enhancer candidates
148 identified from PRO-seq data as enhancers.
149
150 *Gene and Enhancer Transcription Is Precisely Restored after an Acute Heat Shock*
151 A single heat shock induced hundreds and repressed thousands of genes, and caused Pol II to
152 accumulate at transcribed enhancers (Mahat *et al*., 2016; Vihervaara *et al*., 2017; Figure 1A). To
153 address whether this heat-induced reprogramming of RNA synthesis is followed by restoration or
154 readjustment of transcription, we measured nascent RNA synthesis in MEFs upon a 4- or 48-hour
155 recovery from a single 1-hour heat shock (Figures 1 and S1A). We verified that the transiently
156 heat-shocked MEFs continued to proliferate and did not undergo cell cycle arrest or apoptosis
157 (Figure S4A). Moreover, Pol II levels remained constant throughout the experimentation (Figure
158 S4B). Surprisingly, during only a 4-hour recovery, the genome-wide profile of gene body and
159 enhancer transcription was precisely restored to the level observed prior to the heat shock (Figure
160 1A-B). Despite the full recovery of transcription at enhancers and gene bodies, certain promoter-
161 proximal regions gained new pause sites (Figure 1B), or increased Pol II pausing at a single site
162 (Figure S4C-D), during the recovery. Consequently, the genome-wide average of paused Pol II
163 remained elevated, even when measured 48 hours after the heat exposure (Figure 1C).
164
165 *Heat Shock Primes Accelerated Gene Induction over Mitotic Divisions*
166 Individual genes and whole transcription programs can be coordinated at the step of promoter-
167 proximal pause-release (Rougvie and Lis, 1988; Boettiger and Levine, 2009; Mahat *et al*., 2016;
168 Vihervaara *et al*., 2017). To address whether the changed Pol II pausing in daughter cells alters
169 genes' heat responsiveness, we preconditioned MEFs with a single 1-hour heat shock, allowed a
170 48-hour recovery and measured transcription kinetics provoked by an additional heat shock. Instant
171 and sustained changes in heat-induced transcription were assayed with PRO-seq upon 0, 12.5, 25,
172 and 40 minutes of heat shock, and by comparing the transcriptional stress response between
173 unconditioned and preconditioned cells (Figures 2A and S1B). Analyses of productive elongation
174 with DESeq2 (Love *et al*., 2014) showed clear differences in transcription upon 12.5 minutes of
175 heat shock in preconditioned *versus* unconditioned cells (Figure S5A). Several genes, *e.g.*

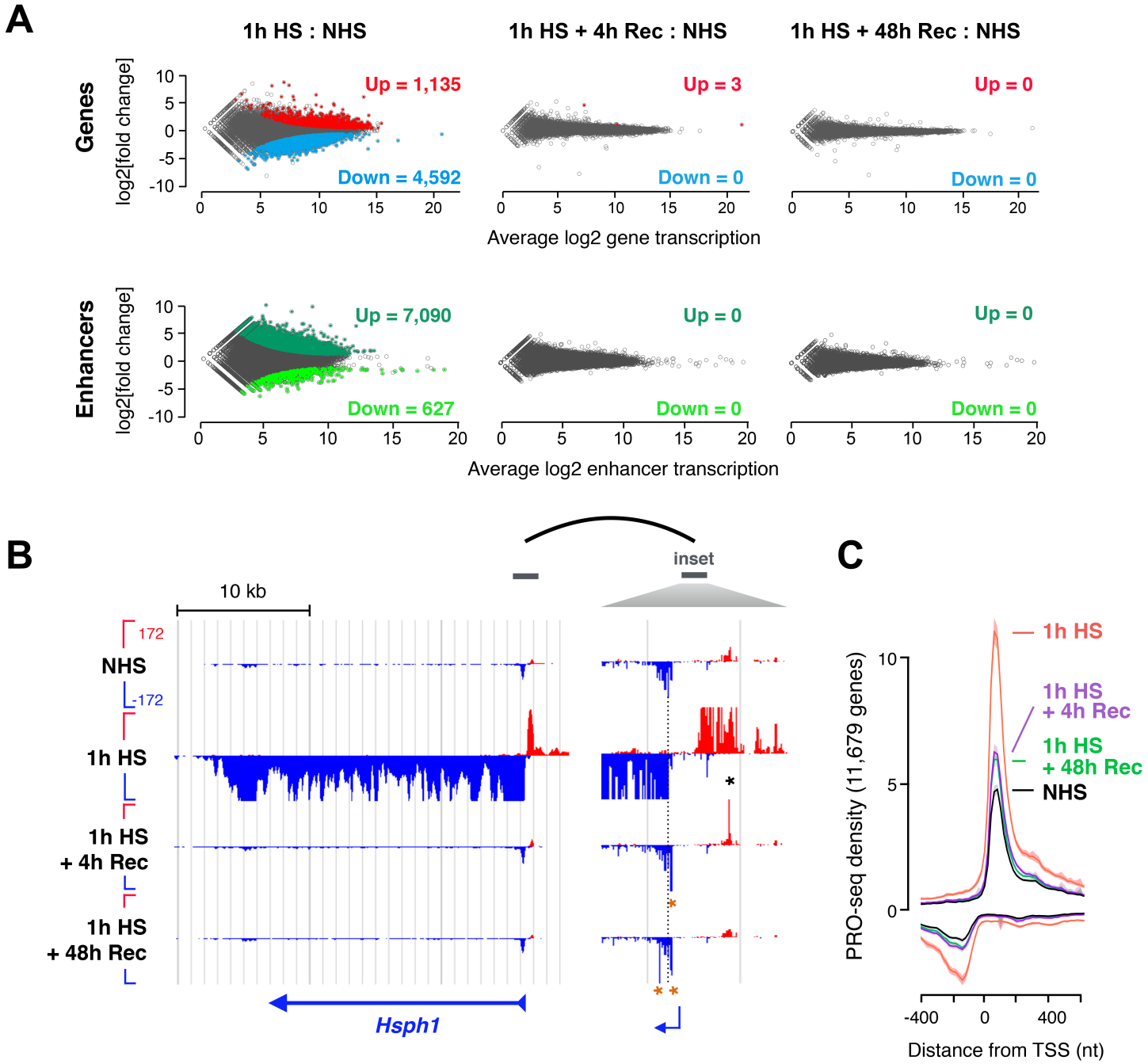

Figure 1. Transcription of genes and enhancers precisely recovers after heat-induced reprogramming. A) DESeq2-analysis of differential gene and enhancer transcription in mouse embryonic fibroblasts (MEFs). Up and Down denote a statistically significant increase or decrease, respectively, in Pol II density at gene bodies (upper panels) and enhancers (lower panels) upon heat shock and recovery, as compared to optimal growth conditions. **B)** Transcriptional profile of a heat-induced *Hsph1* gene in the non-heat-shock condition, upon 1 h of heat shock, and upon recovery from a 1-h heat shock. Inset depicts promoter-proximal region. The dashed line indicates highest Pol II pausing density in non-heat-shocked cells, and asterisks denote prominent Pol II pausing on sense (orange) and anti-sense (black) strand after recovery. **C)** Average promoter-proximal pausing measured at all transcribed genes. Shaded area indicates 12.5 to 87.5% confidence interval. Bin size is 20 nt. HS: heat shock; NHS: non-heat shock; Rec: recovery. The y-axis in B is in linear scale from 172 to -172 for each browser track.

176 polyubiquitin-coding *Ubc* (Figure 2B) and metallothionein *Mt1* (Figure S5B) had gained a faster
177 heat induction by preconditioning, whereas others, *e.g.* serum response factor (*Srf*), displayed a
178 slower heat induction (Figure S5C). At *Ubc*, the promoter-proximal Pol II pausing was elevated
179 after preconditioning (0-min inset in Figure 2B), and the paused Pol II was released faster into
180 elongation upon heat shock (12.5-min inset in Figure 2B). At *Mt1*, prominent Pol II pausing was
181 detected upon 12.5 minutes of heat shock only in unconditioned cells, while in preconditioned cells
182 it was actively elongating at all time points (Figure S5B). Noteworthy is that unconditioned cells
183 also gained efficient Pol II pause-release and high heat-induced transcription after 12.5 minutes of
184 heat shock (Figures 2B, S5A-B), indicating that preconditioning accelerated the onset of heat
185 shock-induced transcription.
186
187 *Faster Pause-Release Accelerates Gene Induction in Preconditioned Cells*
188 More than 400 heat-activated genes displayed an accelerated induction after preconditioning,
189 measured as a significant increase in productive elongation upon 12.5 minutes of heat shock
190 (Figure S5A). To investigate whether the increased Pol II density on the gene bodies could be
191 explained by changes in initiation, pausing, or pause-release, we monitored Pol II progression
192 through the promoter-proximal region. At genes with accelerated induction, the average Pol II
193 pausing was similar between unconditioned and preconditioned cells upon 12.5 minutes of heat
194 shock, but more Pol II had escaped into productive elongation in preconditioned cells (Figures 2C
195 and S5A). In comparison, preconditioning did not change Pol II progression through the pause at
196 genes that were highly (Figure 2C) or early (Figure S5D) heat-induced in unconditioned cells. The
197 faster progression of Pol II through the promoter-proximal region at a subset of genes revealed that
198 preconditioning produces a transcription memory that primes a selected set of genes for a more
199 rapid heat activation.
200
201 A faster entry of Pol II into productive elongation can be accomplished by an accelerated onset of
202 *trans*-activation, as demonstrated at *Ubc* (Figure 2B) and *Mt1* (Figure S5B), or by a faster moving
203 Pol II. At over a 100 kb long *vinculin* (*Vcl*) gene (Figure 2D), the wave of productive elongation
204 extended tens of kb both in unconditioned and preconditioned cells upon a 12.5-minute heat shock,
205 showing an instant *trans*-activation regardless of the preconditioning. Intriguingly, the elongation
206 wave had proceeded farther at *Vcl* in preconditioned cells (Figure 2D), indicative of a faster moving
207 Pol II. In agreement, Pol II density at the pause of *Vcl* (insets in Figure 2D) was lower in
208 preconditioned cells, which demonstrates a shorter residence time of Pol II at the pause region

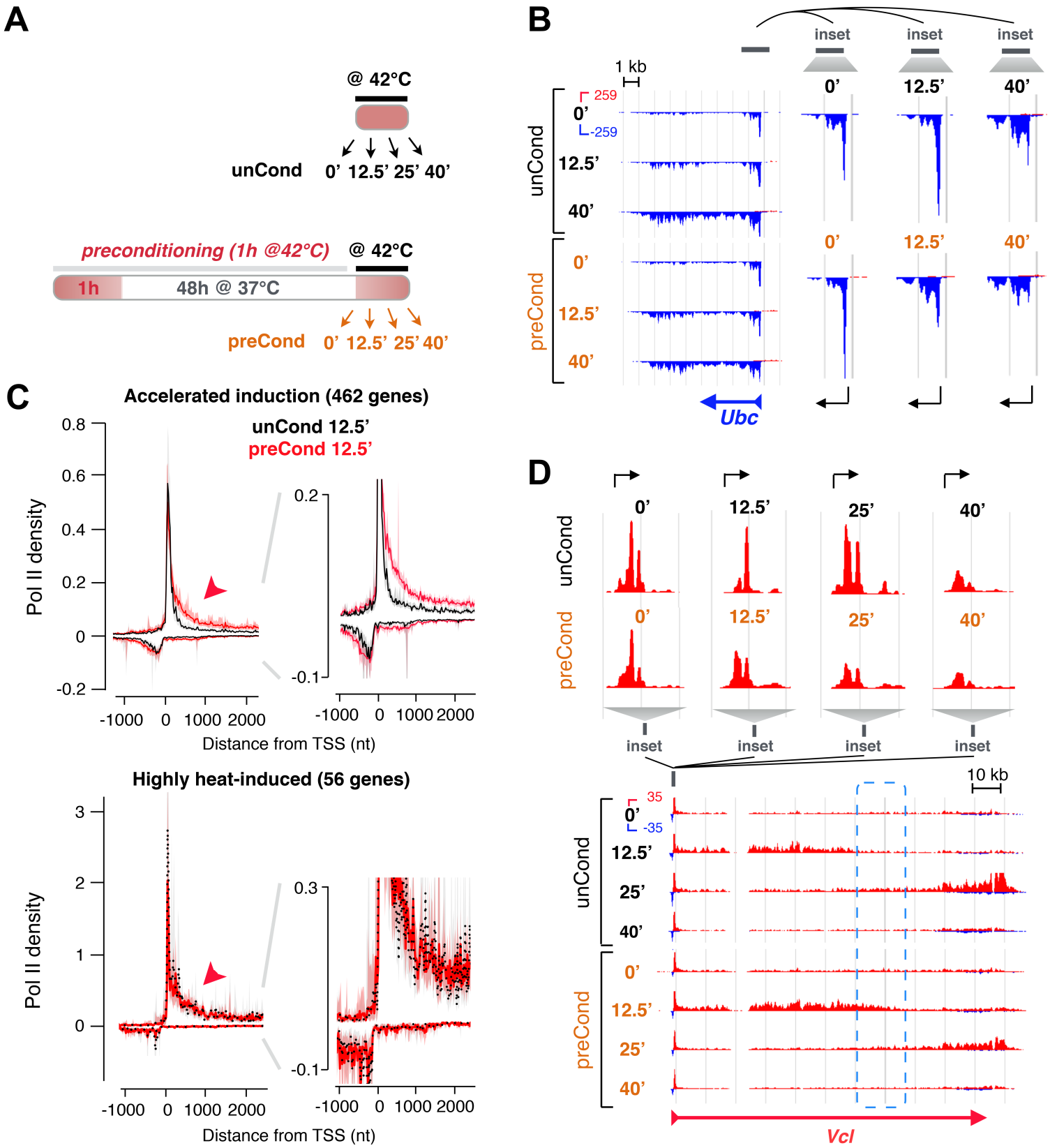

Figure 2. A single heat shock primes accelerated gene-induction over mitotic divisions. A) Experimental setup for measuring transcription kinetics in unconditioned (unCond) and single heat shock-conditioned (preCond) mouse embryonic fibroblasts (MEFs). Transcription was analyzed upon a 0, 12.5, 25 or 40-min heat shock in unconditioned cells (upper panel), and in cells that were preconditioned with a 1-h heat shock and 48-h recovery (left panel). **B)** Nascent transcription at *Ubc* prior to and upon heat shock in unconditioned and preconditioned cells. The insets show Pol II density in promoter-proximal region in unconditioned (upper panels) and preconditioned (lower panels) cells. The grey vertical lines in insets mark 1 kb intervals. **C)** Average intensity of transcription upon a 12.5-min heat shock at the promoter-proximal region of genes that gain a faster heat-induction by preconditioning (upper panel) or at genes that are highly heat-induced regardless of preconditioning (lower panels). Pol II density after the pause-release is indicated with an arrow head. The inset compares Pol II density after the pause-release. Shaded area indicates 12.5 to 87.5% confidence interval. Bin size is 20 nt. **D)** Heat-induced wave of transcription along *Vcl* gene. The blue dashed region indicates an advancing wave of transcription that has proceeded farther in preconditioned than in unconditioned cells upon 12.5 min heat shock. The insets show promoter-proximal Pol II density in unconditioned (upper panels) and preconditioned (lower panels) cells. The grey vertical lines in insets mark 100 nt intervals.

209 before entering into productive elongation. Regardless whether a gene gained accelerated induction
210 due to a faster onset of *trans*-activation, faster moving Pol II through promoter-proximal region
211 and gene body, or their combination, our results uncover the promoter-proximal pause-regulation
212 as a mechanistic step for enabling an accelerated heat induction.
213
214 *Single Heat Shock Preconditioning Accelerates Induction of Quality Control Genes*
215 Genes that gained a faster heat induction by preconditioning were enriched for lysosomal,
216 autophagocytosis and membrane-associated functions (Figure S5E). These genes encode a
217 machinery for clearing damaged organelles and proteins through lysosomal degradation (reviewed
218 in Guido *et al*, 2010). In comparison, genes that were highly or early induced, regardless of the
219 preconditioning, encoded chaperones, cytoskeletal components, and negative regulators of
220 transcription (Figure S5E). Hence, preconditioning MEFs with a single heat shock primed the
221 lysosomal pathway of quality control for instant transcriptional activation, a pathway that
222 complements the chaperone-mediated combating of proteotoxic stress.
223
224 *Human K562 Cancer Cells Restore Basal and Heat-Induced Transcription after a Single Heat*
225 *Shock*
226 Cancer cells live under conditions where both intracellular and extracellular stresses challenge the
227 cells' integrity and proliferation (reviewed in Hanahan and Weinberg, 2011; Chen and Xie, 2018).
228 To understand the transcriptional mechanisms by which cancer cells adapt to stress, we moved
229 from stress-sensitive untransformed MEFs to human K562 erythroleukemia cells. K562 cells are a
230 patient-derived malignant cancer cell line (Lozzio and Lozzio, 1975; Koeffler and Kolde, 1980),
231 known to tolerate extended heat treatments and develop thermotolerance (Mivechi, 1989;
232 Vihervaara *et al*., 2013). Preconditioning K562 cells with a single heat shock recapitulated the
233 instant heat-induced reprogramming of transcription (Figure S6A) and the precise restoration of
234 cell type-specific transcription program upon a 48-hour recovery (Figure S6B), alike MEFs (Figure
235 1A). Furthermore, the daughters of cells exposed to a single heat stress displayed an unaltered
236 stress response by inducing and repressing virtually the same set of genes (Figures S6C and S7A),
237 and with strikingly similar kinetics (Figure S7A-B), as their parental cells. The similar stress
238 responses in unconditioned and singly preconditioned K562 cells may reflect the constitutive stress
239 response in cancer cells (Mivechi 1989; Leppä *et al*., 2001; Chatterjee and Burns, 2017; Klimczak
240 *et al*., 2019).
241

242 *Multiple Heat Shocks Reprogram Basal Transcription in Cancer Cells*

243 Pathophysiological stresses caused by cancer and neurodegeneration are often sustained or
244 repeated. To investigate whether repeatedly encountered stress affects gene and enhancer
245 transcription, we preconditioned K562 cells with a total of nine 1-hour heat shocks during three
246 consecutive days. After a 48-hour recovery, the basal transcription in daughter cells and their
247 transcriptional response to an additional single heat shock was measured (Figure 3A). K562 cells
248 proliferated throughout the six days of preconditioning, recovery and additional heat shock (Figure
249 S8A) without showing signs of apoptosis or increased polyploidy (Figure S8B). PRO-seq datasets
250 were normalized using whole-genome spike-in (Figure S8C-D), and Pol II protein levels were
251 verified to remain constant during the experiments (Figure S8E).

252

253 Following the recovery from nine heat shocks, the vast majority of genes and virtually every
254 enhancer had restored their transcription to a level detected in unstressed cells (Figures 3B and
255 S9A), including lineage-specific regulators GATA and TAL1 (Fujiwara *et al*., 2009; Wu *et al*.,
256 2014; Huang *et al*., 2016). However, preconditioning with several heat shocks caused elevated
257 synthesis of seven genes and reduced synthesis of over 500 genes (Figure 3B-C). The most
258 prominent increase in basal transcription was detected for *HSPA8* (Figure 3C) that encodes HSP70
259 cognate (HSC70), a constitutively expressed chaperone important for protein homeostasis (Ignolia
260 and Craig, 1982; Kampinga *et al*., 2009). Genes with repressed basal transcription encode
261 regulators of protein production and maturation (Figure S9B-C; Supplemental Dataset 1),
262 suggesting a slower protein production in the daughters of repeatedly stressed cancer cells.

263

264 *Repeated Stress Re-Wires Heat-Inducibility*

265 Subjecting the daughters of repeatedly stressed cells to an additional heat shock revealed that some
266 genes had lost, gained or accelerated heat induction due to preconditioning (Figure 3D). One of the
267 genes that had lost heat induction encodes protein phosphatase 1 regulatory subunit 15A
268 (PPP1R15A *alias* GADD34; Figure 3D), which is a key regulator of translation and maintains
269 protein production in stressed cells (Harding *et al*., 2009; Walter and Ron, 2011). Genes with
270 accelerated heat induction included *clusterin* (*CLU*; Figure 3D), a glycosylated chaperone that
271 facilitates autophagy, ameliorates ER-stress, and enhances cancer cell survival (Zhang *et al*., 2014).
272 The few genes that had gained heat induction encode proteins with functions in cell survival and
273 growth arrest (Supplemental Dataset 1). We did not detect activation of apoptotic pathways or
274 changes in cell cycle regulators (Figure S9D; Supplemental Dataset 1). This underscores the

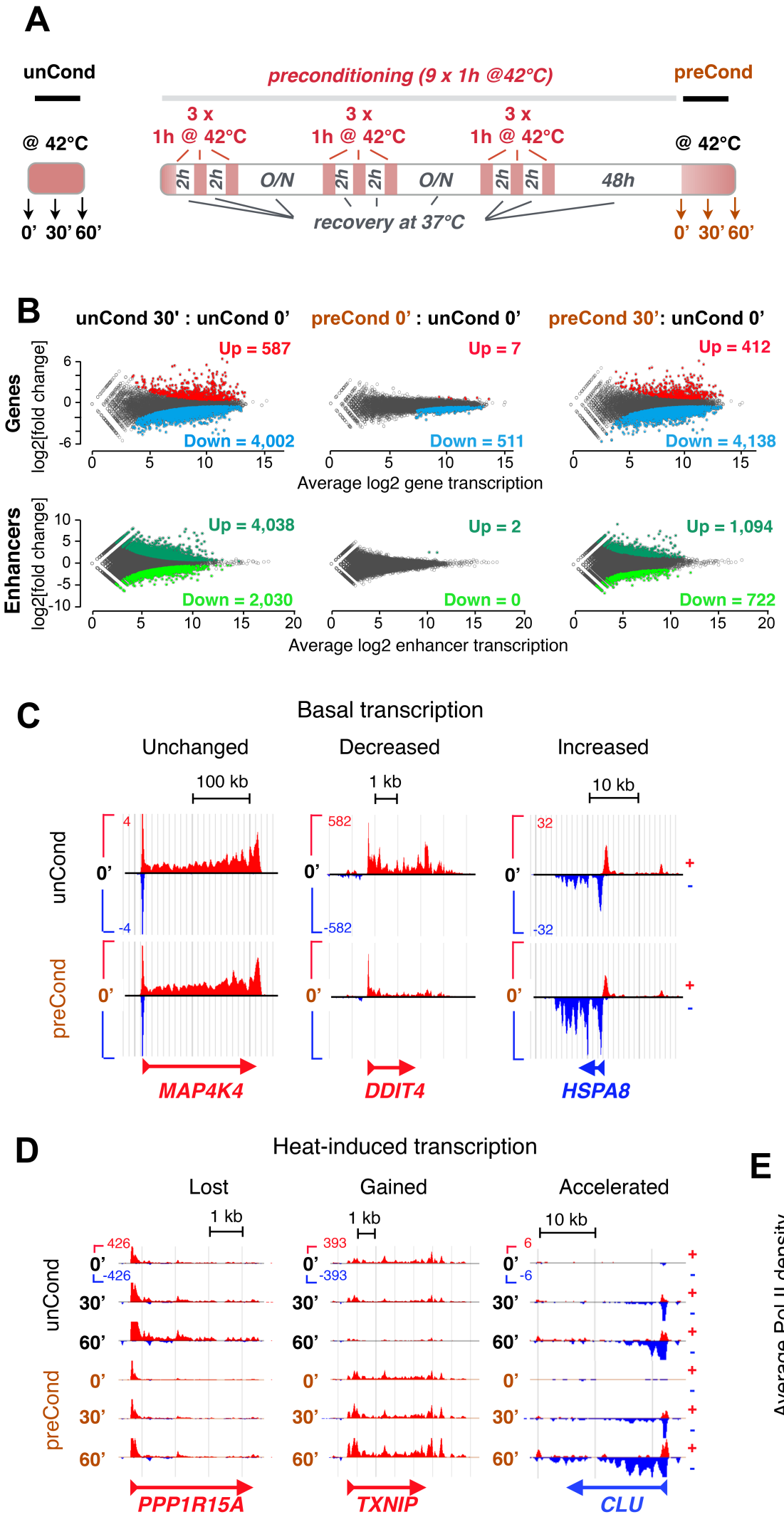

Figure 3. Repeated heat shocks refine basal and inducible transcription in the daughter cells. A) Experimental setup for preconditioning human K562 cells with multiple heat shocks. Genome-wide nascent transcription was measured upon a 0, 30 or 60-min heat shock in unconditioned cells (left panel), and in cells that were pre-exposed to nine 1-h heat shocks during three consecutive days, and allowed to recover for 48 h prior to an additional 1-h heat shock (right panel). **B)** DESeq2-analysis of differential gene and enhancer transcription. Up and Down denote numbers of genes (upper panels) and enhancers (lower panels) with significantly heat-induced or heat-repressed Pol II density, respectively, as measured against non-stressed cells (unCond 0'). **C)** Transcriptional profiles of genes with unchanged (left panel), decreased (middle panel) or increased (right panel) basal transcription due to preconditioning. **D)** Transcriptional profiles of genes that had lost (left panel), gained (middle panel), or accelerated (right panel) heat-induction as a result of preconditioning. **E)** Average Pol II density at promoter-proximal regions of heat-induced genes. Shaded area indicates 12.5 to 87.5% confidence interval. Bin size is 20 nt.

275 survival potential of K562 cancer cells throughout the series of protein-damaging stress (Figure
276 S8A-B), an adaptation that involves altering the transcription program to maintain homeostasis.
277
278 *Repeated Heat Shocks Reduce Initiation and Prolong Termination over Mitotic Divisions*
279 The most striking change in transcription in the daughters of repeatedly preconditioned cells was
280 a global reduction in Pol II density at the promoter-proximal regions of heat-activated genes
281 (Figures 3E and 4A). In PRO-seq, the 3'-end of each read reports the genomic position of
282 transcribing Pol II and it is used for mapping the active sites of transcription. Instead, the 5'-ends
283 of PRO-seq reads are enriched at the initiating base of each transcript, providing a read-out for the
284 usage of transcription start sites (TSSs). Visualizing the 5'-ends of PRO-seq reads revealed that
285 initiation was severely declined at heat-induced genes after preconditioning (Figure 4B). In
286 comparison, distribution of the 3'-ends of PRO-seq reads showed that both the pausing and the
287 pause-release followed a similar course (Figure 4B). The reduction in heat-induced initiation in
288 preconditioned cells occurred concurrently with an increase in Pol II density at the termination
289 window (Figure 4A-D). Indeed, the more actively the gene was transcribed upon heat shock, the
290 more Pol II accumulated at the termination window (rho 0.55) and the less Pol II was engaged at
291 the gene's promoter-proximal region (rho -0.43) in preconditioned cells (Figure 4C). The increased
292 Pol II density in preconditioned cells was confined to 5000 nucleotides (nt) downstream of the
293 cleavage and polyadenylation site (CPS; Figure 4D). This local confinement of Pol II at the
294 termination window differs from previously described run-through transcription that has been
295 detected under stress conditions (Vilborg *et al*., 2017). While the run-through transcription can
296 extend tens of kb downstream of CPS (median 8.9 kb) and does not locally confine Pol II to CPS
297 (Vilborg *et al*., 2017; Figure S9D), the daughters of repeatedly preconditioned cells accumulated
298 Pol II at the termination window (Figure 4A-D).
299
300 *Chromatin Accessibility Spreads from Primed Promoters to Heat-Induced Genes*
301 Promoter architecture primes genes for heat activation (reviewed in Vihervaara *et al*., 2018), and
302 changes in epigenetic landscape have been coupled to transcriptional memory (reviewed in D'Urso
303 and Brickner, 2017). To study whether the compromised Pol II progression through genes in
304 repeatedly stressed cells was coupled to altered chromatin accessibility, we performed ATAC-seq
305 (Buenrostro *et al*., 2013) in unconditioned, singly preconditioned and repeatedly preconditioned
306 K562 cells (Figures S10-11A). Measuring chromatin accessibility prior to and upon heat shock
307 revealed that chromatin accessibility spread with transcription into heat-induced genes, and that

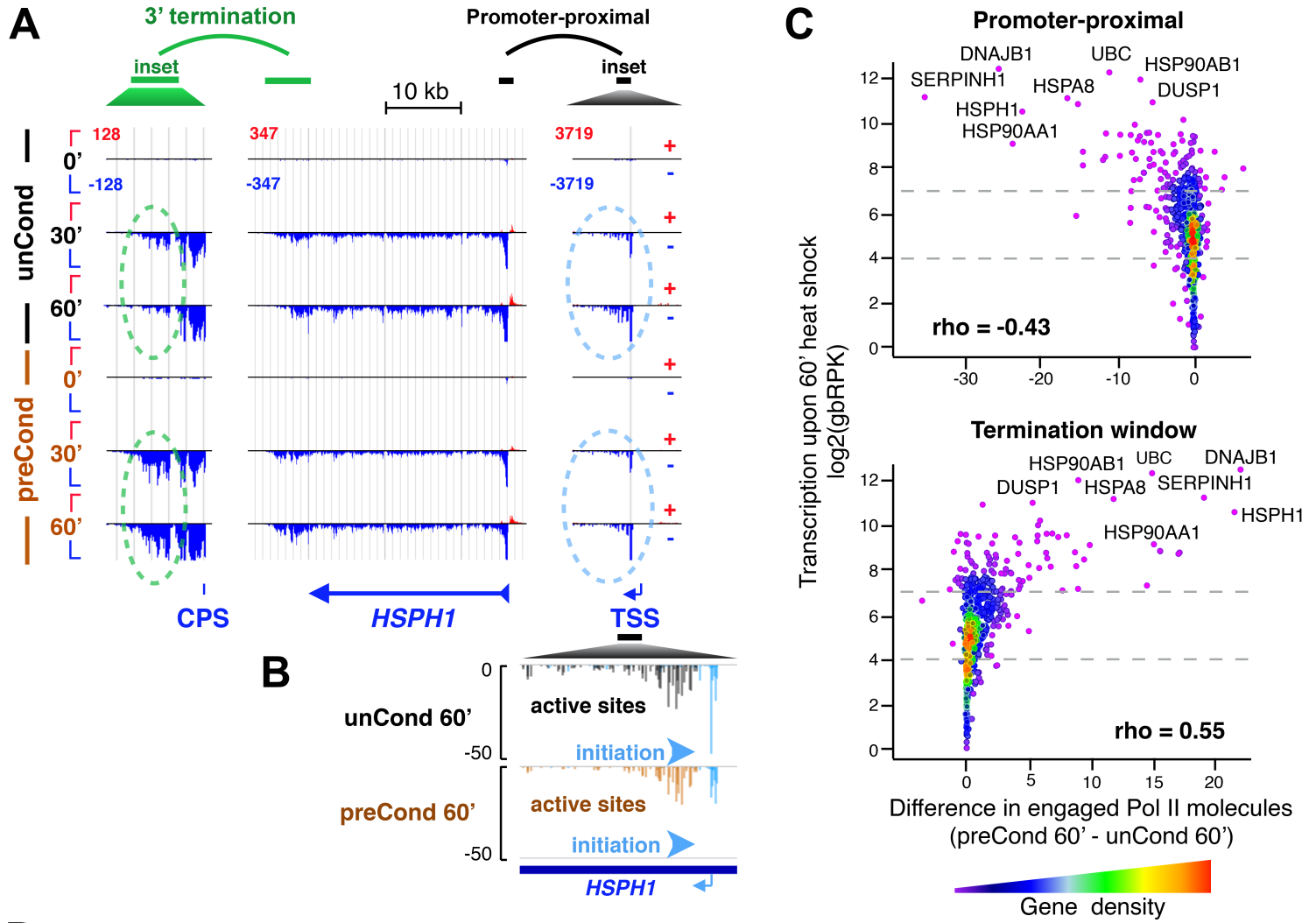

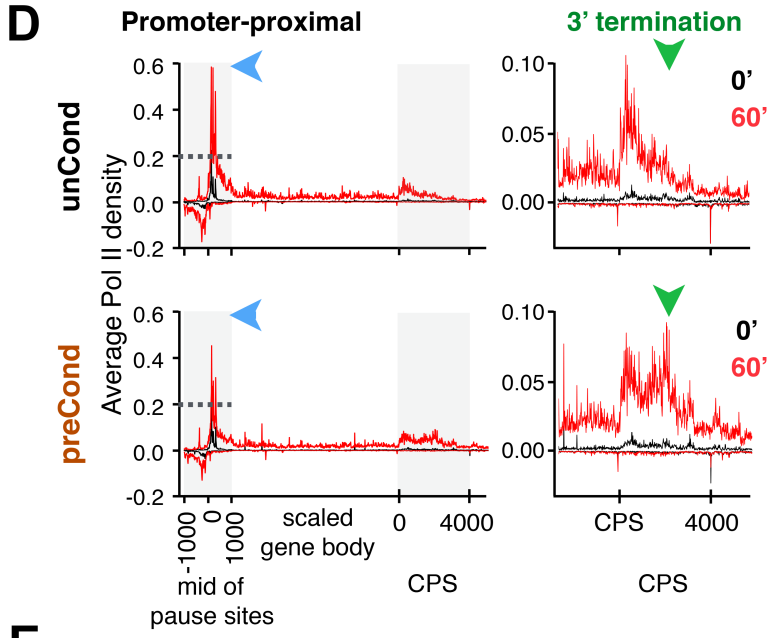

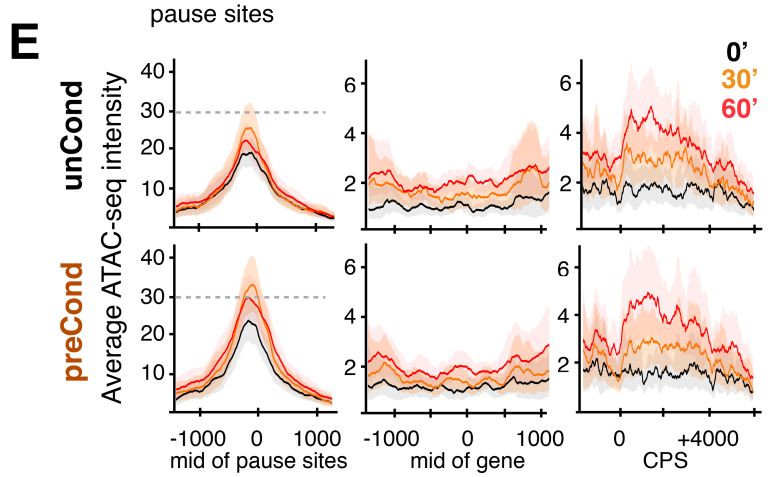

Figure 4. Initiation is reduced and termination prolonged in the daughters of repeatedly stressed K562 cells. A) Nascent transcription along *HSPH1* showing reduced density of engaged Pol II at the promoter-proximal region (light blue dashed circle) and increased density downstream of the Cleavage and Polyadenylation Site (CPS; green dashed circle) in preconditioned cells. **B)** Promoter-proximal region of *HSPH1* showing active sites of transcription (3'-end of each PRO-seq read), and initiation intensity (5'-end of each PRO-seq read). The arrowheads compare the intensity of initiation, the arrow denotes transcription initiation site upon heat shock. **C)** Transcriptional activity of heat-induced genes (n=587) compared with the change in Pol II density at promoter-proximal region (0 to +1000 from the TSS, upper panel) or termination window (+100 to +6000 from the CPS, lower panel) due to preconditioning. Spearman's rank correlations (rho) and the most affected genes are indicated. **D)** Average density of engaged transcription complexes along highly heat-induced genes in unconditioned (upper panels) and preconditioned (lower panels) cells. The light blue arrowheads indicate the promoter-proximal Pol II, the green arrowheads show the site of increased Pol II engagement in preconditioned cells. **E)** Average ATAC-seq density at highly heat-induced genes in unconditioned (upper panels) and preconditioned (lower panels) cells. Shaded area indicates 12.5 to 87.5% confidence interval. Bin size is 20 nt.

308 upon recovery, the chromatin accessibility was restored to pre-stress levels (Figures 4E, S11B-C
309 and S12A). However, ATAC-seq found only minor, if any, changes in the chromatin due to
310 preconditioning (Figures 4E, S11B-C, S12A-D). Particularly, at genes with the highest heat
311 induction, the difference in Pol II densities was pronounced between unconditioned and repeatedly
312 preconditioned cells (Figure 4D), but the corresponding average ATAC-seq densities showed no
313 significant differences (Figure 4E). Only a few genes with the most remarkable changes in Pol II
314 progression displayed minor changes in chromatin accessibility due to preconditioning (Figures
315 S11B-C and S12C-D).
316
317 Chromatin state could change without detectable differences in transposase accessibility.
318 Therefore, we performed MNase-coupled chromatin immunoprecipitation (MNase-ChIP; Skene
319 and Henikoff, 2015) to quantify the levels of histones H2.AZ, H3 and H4, as well as histone H4
320 acetylation (H4ac) at the promoters and +1 nucleosomes of *HSPA1A* and *HSPH1*. In accordance
321 with our ATAC-seq results and previous studies (Petesch and Lis, 2008; Mueller *et al*., 2017),
322 chromatin accessibility increased at the +1 nucleosomes upon stress-induced activation (Figure
323 S12E-F). However, we did not find clear differences in the histone levels between unconditioned
324 and repeatedly preconditioned cells either under basal or heat-induced conditions (Figure S12E-F).
325
326 *Reduced Initiation in Preconditioned Cells Occurs in the Presence of HSF1*
327 Heat-induced *trans*-activation of primed genes requires strong transcription factors, such as HSF1
328 (reviewed in Vihervaara *et al*., 2018). To investigate whether a deficiency in HSF1 reduced
329 initiation at heat-induced genes, we analyzed the expression and DNA-binding ability of HSF1.
330 The transcription (Figure S13A), mRNA expression (Figure S13B) and protein levels (Figure
331 S13C) of HSF1 were comparable in unconditioned and repeatedly preconditioned K562 cells. The
332 binding of HSF1 to the promoters of *HSPA1A* and *HSPH1* was also similar in unconditioned and
333 preconditioned cells (Figures 5A and S13D). Despite the uncompromised capacity of HSF1 to bind
334 to its *cis*-acting elements, the RNA synthesis of *HSPA1A* and *HSPH1* was severely reduced, as
335 were the levels of their corresponding mature mRNAs in preconditioned cells (Figures 5A and
336 S13D). These results coupled the reduced initiation of heat-activated genes (Figure 4A-D) to their
337 lower mRNA expression (Figures 5A and S13D). Furthermore, the reduced initiation in an open
338 chromatin environment and in the presence of a potent *trans*-activator, manifested that the key step
339 for decreased heat activation resided upstream of the promoter architecture and HSF1 binding, *i.e.*
340 at the level of Pol II recruitment.

341

342 *Initiation and Chromatin Opening Are Abated at Heat-Induced Enhancers after Preconditioning*

343 We depleted K562 cells of HSF1 (Figure 5B) and identified over 200 genes and close to 500
344 enhancers that were heat-induced in an HSF1-dependent manner (Figures 5C-F and S13E-F). In
345 addition to *trans*-activating genes by binding to their promoters (reviewed in Vihervaara and
346 Sistonen, 2014), the ability of HSF1 to *trans*-activate genes from enhancers became evident. At the
347 *Tax1 binding protein 1* (*TAX1BP1*) locus, HSF1 only bound to a divergently transcribed enhancer
348 4.5 kb upstream of the promoter (Figure 5C-D), but it was essential for the heat-induced eRNA
349 transcription and for the release of paused Pol II from the *TAX1BP1* promoter (Figure 5C-E).
350 Imporatantly, in repeatedly preconditioned cells, the heat-induced recruitment of Pol II to the
351 HSF1-dependent enhancers was diminished (Figure 5F), uncovering a globally decreased initiation
352 at heat-induced promoters and enhancers (Figures 4C-D and 5C-F). The reduced transcription at
353 HSF1-dependent enhancers after preconditioning was recapitulated in the ATAC-seq data (Figure
354 5G); Transcription-coupled chromatin opening did not occur at HSF1-activated enhancers in
355 repeatedly preconditioned cells, while it was detected in unconditioned and singly preconditioned
356 cells (Figures 5G and S14). In comparison, highly transcribed enhancers showed similar chromatin
357 accessibility regardless of preconditioning or heat shock (Figures 5G and S14).

358

359 *Pol II Accumulates at the Termination Window of Actively Transcribed Genes*

360 The reduced initiation in preconditioned cells prompted us to quantify the distribution of
361 transcription complexes across the genome. We counted engaged Pol II molecules at distinct
362 genomic regions (Figure S15A-B) and found an accumulation of Pol II at the termination window
363 of actively transcribed genes (Figure S15B-E). Over 400 genes simultaneously reduced
364 engagement of Pol II at the promoter-proximal region and increased Pol II engagement at the
365 termination window in the daughters of repeatedly stressed cells (Figure S15D). These genes were
366 characterized by high nascent transcription upon heat shock and included many heat-repressed
367 genes that retained active transcription during heat stress (Figure S15B-E).

368

369 *Repeated Heat Shocks Reduce Transcript Cleavage and Recycling of Pol II*

370 To understand why Pol II accumulated downstream of CPS in preconditioned cells, we examined
371 the processing of transcripts at the termination window. At CPS, the nascent transcript is cleaved,
372 exposing an uncapped 5'-end of the RNA (Figure 6A). The uncapped 5'-end of the nascent
373 transcript is then targeted by exonuclease XRN2, which chases down Pol II and terminates

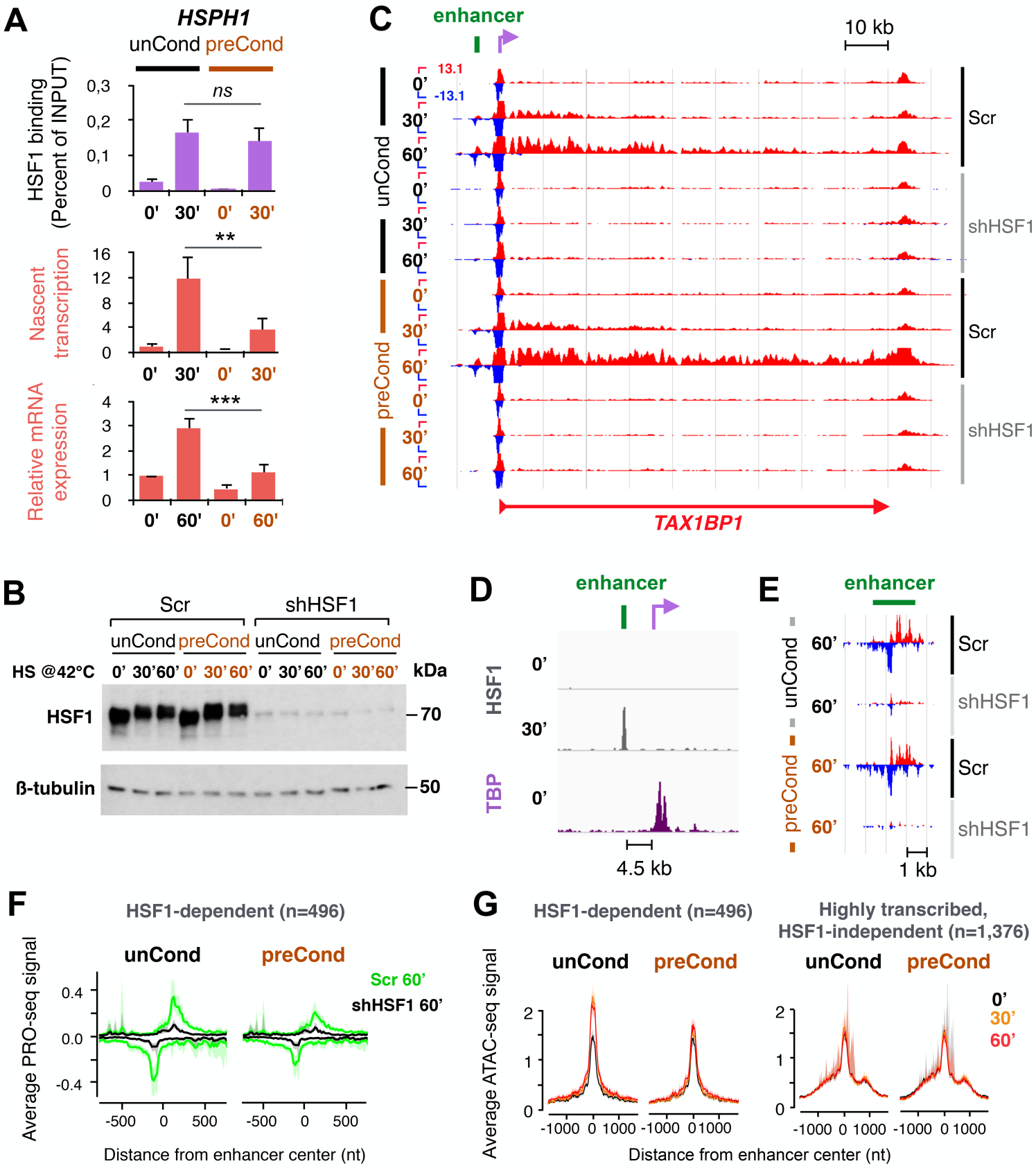

Figure 5. HSF1 *trans*-activates genes *via* promoters and enhancers. A) HSF1-binding intensity to the *HSPH1* promoter (uppermost panel), nascent transcription of *HSPH1* as measured from the first intron (middle panel), and relative level of polyA-containing *HSPH1* mRNA (bottom panel) in unconditioned and preconditioned K562 cells. ** indicates p-value < 0.05 and *** p-value < 0.005. **B)** HSF1 protein expression in scrambled-transfected (Scr) and HSF1-depleted (shHSF1) K562 cells. **C-E)** HSF1 drives heat-induced transcription of *TAX1BP1* gene *via* an upstream enhancer. **C)** Transcription of *TAX1BP1* and its upstream enhancer in the presence and absence of HSF1. **D)** Inset of *TAX1BP1* enhancer (green bar) and TSS (purple arrow), showing heat-induced HSF1 binding (gray) to the enhancer, and TBP binding to the promoter (purple). **E)** Inset showing enhancer transcription in the presence and absence of HSF1 in unconditioned and preconditioned cells upon a 60-min heat shock. **F)** Average Pol II density at HSF1-dependently heat-induced enhancers in the presence (Scr) and absence (shHSF1) of HSF1. **G)** Average ATAC-seq density at HSF1-dependent and highly transcribed enhancers. In F and G, the shaded area indicates 12.5 to 87.5% confidence interval, and bin size is 20 nt. TBP: TATA box Binding Protein. ChIP-seq data for TBP was obtained from ENCODE (Consortium EP, 2011) and for HSF1 from Vihervaara *et al.* (2013).

374 transcription (reviewed in Proudfoot, 2016; Wissink *et al*., 2019). Thus, mapping the 5'-ends of
375 Pol II-associated transcripts at the termination window can provide a read-out for transcript
376 cleavage (Figure 6A). For example, the robustly heat-induced *DNAJB1* gene displayed a clear
377 decrease in initiation and a profound accumulation of Pol II at the termination window after
378 preconditioning (Figure 6B-C). In unconditioned cells, the 5'-ends of PRO-seq reads demonstrated
379 a prominent cleavage at the annotated CPS of *DNAJB1* (Figure 6C). In preconditioned cells, the
380 cleavage site had shifted downstream to a single site at the end of the termination window (Figure
381 6C), and this site occurred at the region of increased Pol II density (Figure 6B).
382
383 We investigated whether reduced cleavage at the termination window could cause the global
384 change in Pol II distribution by analyzing initiation and cleavage at the genes that displayed a
385 prominent change in Pol II progression (Figure 6D). Paused Pol II at the promoter-proximal region
386 has transcribed through fewer nucleotides (<60 nt) than the sequenced read length in our PRO-seq
387 data (75 nt). Thus, the TSS-containing reads report both the initiating base (5'-end of the read) and
388 the position of Pol II at the pause region (Rasmussen *et al*. 1993; Nechaev *et al*., 2010; Tome *et*
389 *al*., 2018), and allows deducing whether Pol II resides at the pause or has proceeded into productive
390 elongation (Figure 6D upper left panel). The decrease in promoter-proximal Pol II in
391 preconditioned cells comprised of transcripts with the whole spectrum of PRO-seq read lengths
392 (20-75 nt), which indicates less initiating, pausing and early elongating Pol II complexes (Figure
393 6D). This reduction in all promoter-proximal Pol II states corroborates our analyses at individual
394 genes where Pol II recruitment was found as the major rate-limiting step of decreased transcription
395 in preconditioned cells (Figures 4B and 6C). At the region downstream of CPS, the read length
396 provides a measure of transcript cleavage: Reads shorter than the maximum sequenced read length
397 contain transcripts that have been cleaved to release the pre-mRNA (Figure 6D upper right panel).
398 The genome-wide increase in Pol II density at the termination window (Figures 4C-D and S15A-
399 D) comprised almost exclusively of reads with the maximum read length (Figure 6D). This
400 selective increase in transcription complexes with no signs of cleavage indicated that the
401 accumulation of Pol II at CPS co-occurred with reduced pre-mRNA processing. Moreover, the
402 reduction in a gene's initiation strongly correlated with the Pol II accumulation at its termination
403 window (p=-0.51, rho=-0.29; Figure S15F), coupling the prolonged termination to the same gene's
404 lower rate of initiation. Since transcript cleavage is required to release Pol II from the chromatin,
405 a compromised recycling of Pol II from the end of the gene into a new initiation could account for
406 the global change in transcription in preconditioned cells.

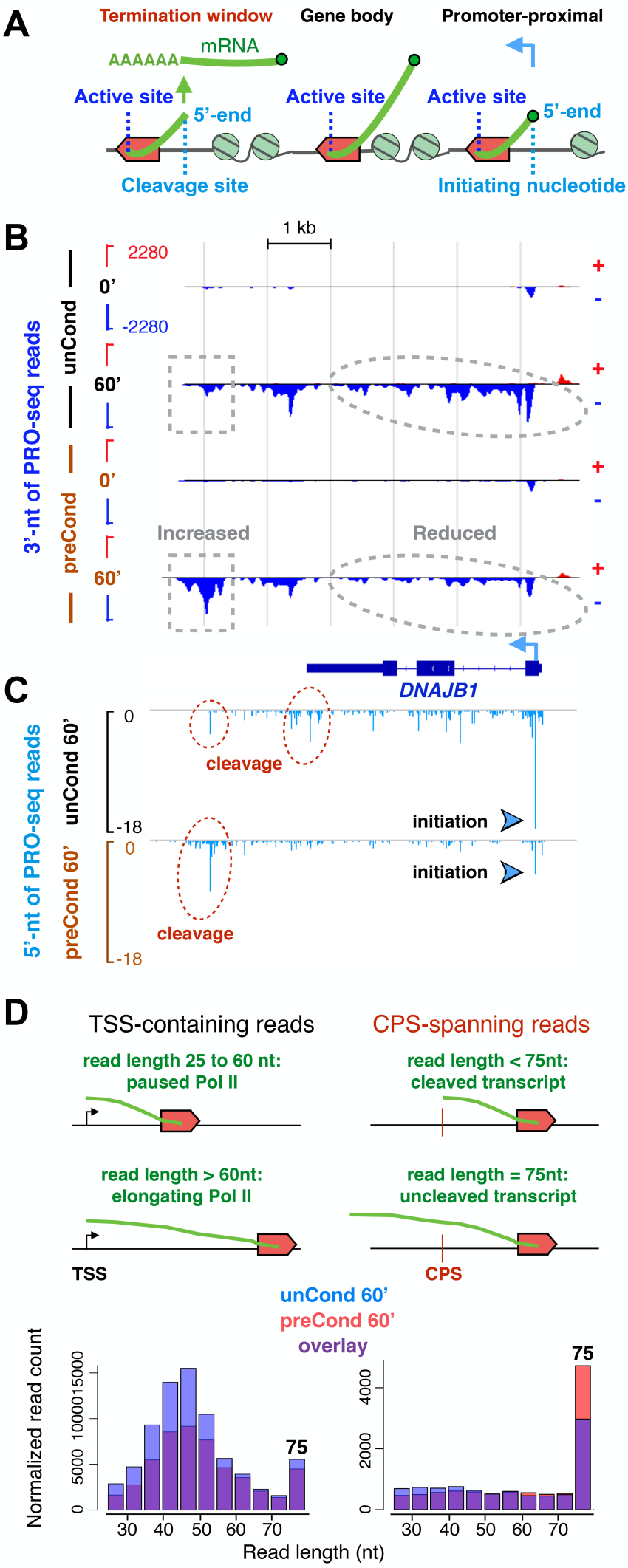

Figure 6. Prolonged termination co-occurs with decreased RNA-cleavage and reduced recycling of Pol II to the gene's promoter and connected enhancers. A) Schematic: 3'-nts of PRO-seq reads report the active sites of transcription, while 5'-nts provide a read-out for initiation (promoter-proximal region) and transcript cleavage (termination window). Pol II is depicted as a red rocket going from right to left. Green sphere in the end of the RNA molecule indicates 5'-cap that protects the transcript from exonucleosomal degradation. **B)** Active sites of transcription (3'-nts of PRO-seq reads) at *DNAJB1* gene. The boxed areas compare heat-induced transcription in unconditioned and repeatedly preconditioned K562 cells. **C)** 5'-nts of PRO-seq reads along *DNAJB1*. Initiation is indicated with light blue arrowheads, transcript cleavage sites are denoted with dashed red circles. **D)** Upper left panel: schematic presentation of TSS-overlapping PRO-seq reads. Paused Pol II associates with 25 to 60 nt long reads, while productively elongating Pol II has proceeded beyond the +60 nt from the TSS. Lower left panel: lengths of TSS-overlapping PRO-seq reads at genes where Pol II progression changes due to preconditioning (n=429). The reduction of promoter-proximal Pol II in repeatedly preconditioned cells consist of paused (25 to 60 nt long reads) and early elongating (>60 nt long reads) transcription complexes. Upper right panel: schematic representation of CPS-overlapping PRO-seq reads. Reads shorter than the maximum read length (here 75 nt) report events of transcript cleavage. Lower right panel: lengths of CPS-spanning reads at genes with a changed Pol II progression (n=429). Accumulated Pol II molecules in termination windows of repeatedly preconditioned cells associate with uncleaved transcripts. **E)** Fold change of engaged Pol II in preconditioned over unconditioned cells at termination windows, promoter-proximal regions, and connected enhancers. The red dashed line indicates fold change 1. Increased and decreased denote higher and lower, respectively, Pol II density after preconditioning.

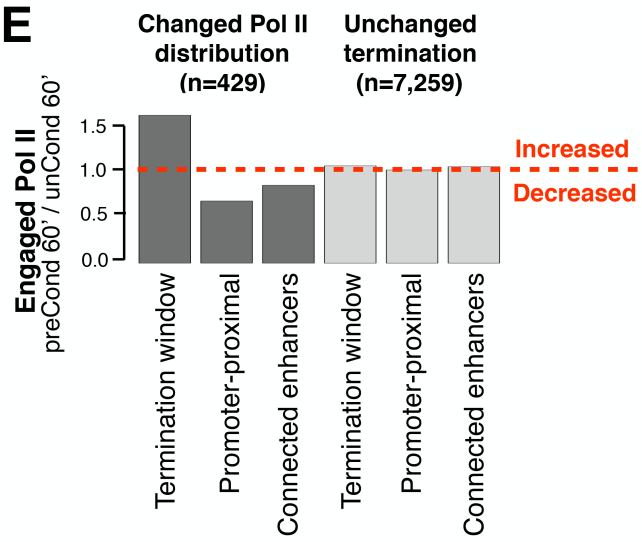

407

408 *Enhancers with Reduced Initiation Connect to Genes with Increased Pol II Density at the*
409 *Termination Window*

410 Enhancers recruit transcription factors and Pol II, and they are brought to physical proximity with
411 the target genes *via* chromatin looping (reviewed in Field and Adelman, 2020). To analyze
412 recycling of Pol II between genes and enhancers, we identified chromatin loops and measured Pol
413 II density at the connected genes and enhancers. Enhancers that looped to genes with increased Pol
414 II density at the termination window showed a significant reduction in heat-induced Pol II density
415 after preconditioning (Figures 6E and S15G). In contrast, enhancers that looped to genes without
416 a prominent change in the termination displayed similar Pol II densities in unconditioned and
417 preconditioned cells (Figures 6E and S15G). Monitoring the progression of Pol II through the
418 distinct rate-limiting steps of transcription allows us to propose a model (Figure 7) where reduced
419 transcript cleavage at the termination window retains Pol II bound to chromatin and diminishes
420 recycling of the transcription machinery. The limited availability of Pol II in preconditioned cells
421 lowers initiation without the need to change the chromatin state or HSF1-binding. The lower
422 initiation rate, in turn, reduces mRNA production in preconditioned cells. Our model also explains
423 the lower enhancer transcription in preconditioned cells, identifying the affected enhancers to
424 reside in chromatin loops with genes where Pol II accumulates at the termination window.

Heat shock response:

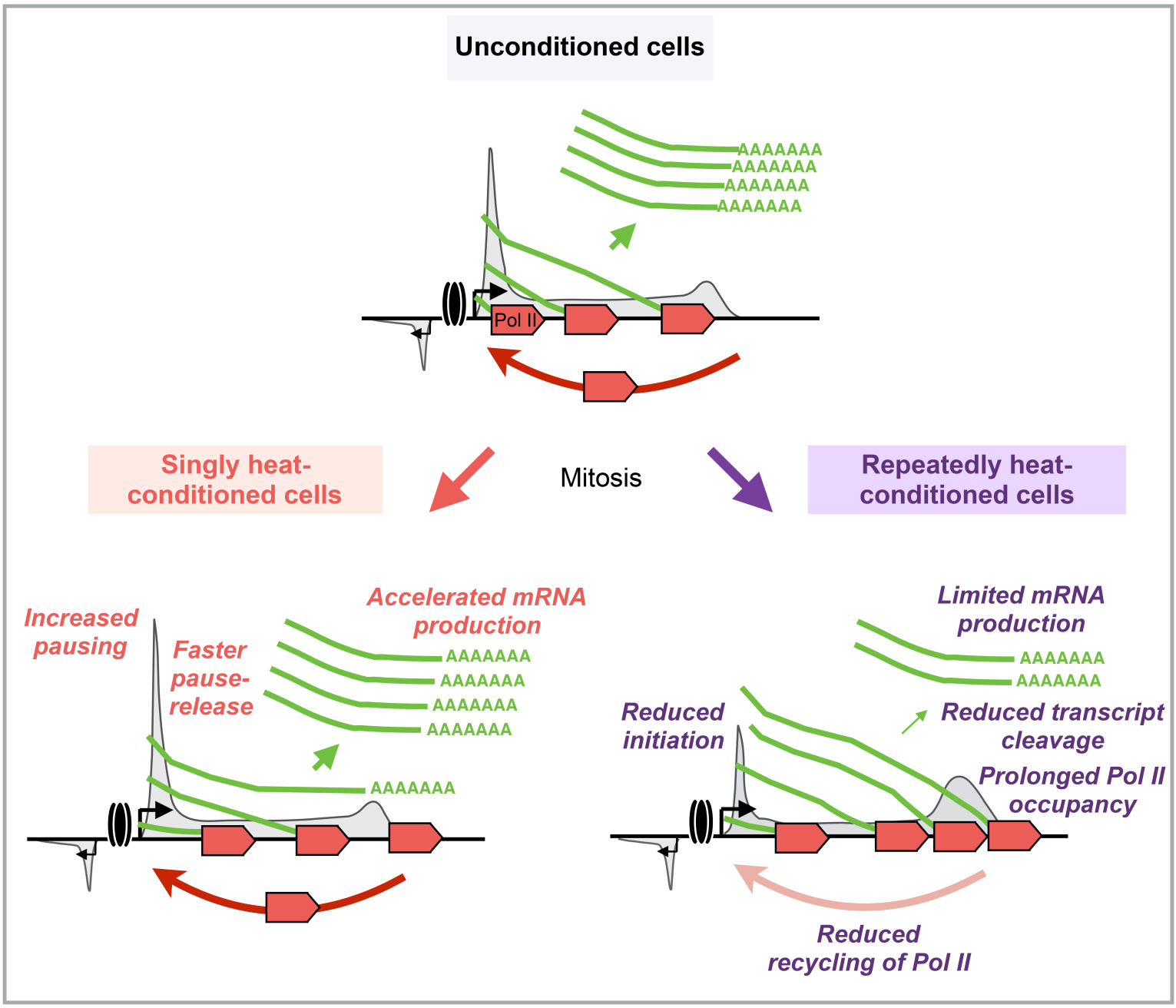

Figure 7. Model for heat-induced transcriptional memory accelerating promoter-proximal pause-release and decelerating termination over mitotic divisions. In unconditioned cells (upper panel), paused Pol II is rapidly released from the promoters of heat-induced genes into elongation, and it efficiently proceeds through the gene. A single heat shock exposure (lower left panel) primes an additional set of genes for instant heat-induction in the daughter cells by increasing Pol II pausing and by triggering a more rapid release of Pol II into productive elongation. Multiple heat shocks (lower right panel) cause reduced transcript cleavage at the 3'-end of active genes, which decelerates termination, and decreases recycling of the transcription machinery to heat-activated genes and enhancers.

425 **Discussion**

426

427 *Control of Pol II Pause-Release Enables Rapid and Reversible Transcriptional Reprogramming*

428 The groundbreaking model by Conrad Waddington (1957) describes developing cells as marbles
429 that roll down an energy landscape of hills and valleys. While rolling down, cells take different
430 paths and commit to distinct cell types, remodeling their chromatin environment and transcription
431 program (reviewed in Takahashi and Yamanaka, 2015). Reversing from a differentiated to
432 pluripotent cell, instead, requires specific transcription factors that push the cell up the energy
433 landscape, which rarely occurs in nature (Gurdon *et al*., 1958; Takahashi and Yamanaka 2006).
434 Here, we showed that after genome-wide reprogramming of transcription by heat shock, cells
435 return to their cell type-specific transcription program within hours of recovery (Figure 1). In
436 Waddington's landscape, the heat-induced reprogramming would be analogous with the cell
437 transiently occupying a near-by valley, but during recovery, returning to its cell type-specific basal
438 transcription program. This rapid reprogramming and precise recovery highlight the plasticity of
439 transcription program and implies that the transcriptional heat shock response is truly transient.

440

441 The rapid and reversible heat-induced reprogramming can be explained mechanistically by
442 genome-wide control of promoter-proximal Pol II pause-release. An important consequence of
443 repressing thousands of genes by preventing the release of Pol II from their promoter-proximal
444 regions is its rapid reversibility; a simple reactivation of the pause-release can restore productive
445 gene transcription throughout the genome without extensive chromatin remodeling. In this regard,
446 Pol II pausing can be considered as a memory that marks active genes and maintains open and
447 accessible promoters during their transient repression. Indeed, reprogramming of transcription
448 during differentiation involves gene silencing and activation by remodeling the chromatin
449 (reviewed in Perino and Veenstra, 2016; Gökbuget and Blelloch, 2019). The reported changes in
450 the chromatin upon heat shock (Zobeck *et al*., 2010; Petesch and Lis, 2012, Niskanen *et al*., 2015,
451 Mueller *et al*, 2017; Vihervaara *et al*, 2017) involve modifications that are likely to transiently
452 compartmentalize distinct gene activities (reviewed in Vihervaara *et al*., 2018). Moreover,
453 chromatin conformation remains stable upon heat shock (Ray *et al*., 2019), which implies that the
454 rapid recovery from stress does not require rewiring of the chromatin connectivity. We conclude
455 that as chromatin architecture is primed for an instantaneous transcriptional response to heat shock
456 (Vihervaara *et al*., 2017; Ray *et al*., 2019), the Pol II pausing at heat-repressed genes primes rapid
457 and robust transcriptional recovery, providing a memory of the cell's transcription program.

458

459 *Stress-Induced Control of Pol II Is Carried over Mitotic Divisions*

460 A single heat shock, which is unlikely to cause permanent or long-lasting damage to the cell, did
461 not change the basal transcription but increased Pol II pausing (Figure 1). The pausing of Pol II, in
462 turn, can function as a space-holder for a rapid signal-responsive regulation. In accordance, the
463 daughter cells of singly preconditioned MEFs were able to accelerate Pol II entry into productive
464 elongation (Figure 2). The faster induction of the machinery that clears damaged proteins and
465 organelles *via* lysosomal degradation (Figure 7) is likely to raise another instant cytoprotective arm
466 next to the rapidly heat-induced chaperone expression.

467

468 Cancer cells are highly stress-tolerant (Hanahan and Weinberg, 2011). Accordinly, human K562
469 erythroleukemia cells proliferated through multiple heat shocks and adapted nascent transcription
470 program to support survival. Two mitotic divisions after nine heat exposures, transcription of
471 certain pro-survival genes was elevated, expression of genes that maintain protein production was
472 decreased (Figures 3), and processing of transcripts at the 3'-ends of active genes was decelerated
473 (Figure 6). In cells with decreased protein synthesis, the decelerated transcription termination likely
474 serves to reduce the mRNA load as fewer Pol II molecules become available for new rounds of
475 heat-induced transcription (Figures 6-7). The increased association of uncleaved transcripts at the
476 3'-ends of genes could provide a reservoir of pre-mRNAs that are rapidly processed to mature
477 mRNAs once the cell restores its protein synthesis. Our results demonstrate that priming a faster
478 gene activation and refining transcription over mitotic divisions can occur *via* regulation of Pol II
479 (Figures 2-4), without involving major changes in chromatin accessibility or binding-activity of
480 HSF1 (Figures 4 and 5). Taken together, cells exposed to stress can establish a memory by
481 regulating the key rate-limiting steps of transcription.

482

483 *Limitations*

484 This study tracks the process of nascent transcription at genes and enhancers across the genome,
485 and identifies the rate-limiting steps involved in establishing a transcriptional memory of cellular
486 stress. Nevertheless, the factors that execute the increased Pol II pausing and trigger a faster release
487 of the paused Pol II in the daughters of stress-exposed cells remain to be identified. Likewise, the
488 molecular machinery at the termination window that is involved in retaining Pol II associated with
489 the nascent transcript are currently unknown. Increased residency of Pol II at the termination
490 window correlated with reduced initiation at the gene's TSS and connected enhancers. The

491 movements of Pol II between genes and enhancers remain to be shown. The memory-induced
492 changes in Pol II regulation can occur without major changes in chromatin accessibility, but our
493 results do not exclude the involvement of transcriptional regulators in priming a faster
494 transcriptional response to stress or coordinating prolonged termination in the daughters of heat-
495 shocked cells.
496
497 **Competing Interests**
498 The authors declare no competing interests.
499
500 **Author Contributions**
501 A.V., J.T.L. and L.S. conceived and designed the study. A.V., D.B.M., S.V.H. and M.A.H.B.
502 conducted the laboratory work, and A.V. and D.B.M. performed the computational data analyses.
503 All the authors interpreted the results. A.V., J.T.L. and L.S. wrote the manuscript with edits from
504 D.B.M., S.V.H. and M.A.H.B.
505
506 **Acknowledgements**
507 We thank the members of the Sistonen and the Lis laboratories for valuable advice during the
508 manuscript preparation. This work was financially supported by the Sigrid Jusélius Foundation
509 (A.V., L.S.), Academy of Finland (A.V., L.S.), SciLifeLab (A.V), Svenska Tekniska
510 Vetenskapsakademin i Finland (A.V.), South-West Finland's Cancer Foundation (A.V.), Borg
511 Memory Foundation (A.V.), Åbo Akademi University (A.V., L.S.), The Finnish Cultural
512 Foundation (A.V.), Alfred Kordelin Foundation (S.V.H.), Cancer Foundation Finland (L.S.),
513 Magnus Ehrnrooth Foundation (L.S.), and NIH grants RO1-GM25232 and HG009393 (J.T.L.).
514 The content is solely the responsibility of the authors and does not necessarily represent the
515 official views of the National Institutes of Health.
516
517 **Figure Legends**
518
519 **Figure 1. Transcription of genes and enhancers precisely recovers after heat-induced**
520 **reprogramming. A)** Differential gene and enhancer transcription upon heat shock and recovery in
521 MEFs. Up and Down denote a statistically significant increase or decrease in Pol II density at gene
522 bodies (upper panels) and enhancers (lower panels). **B)** Transcriptional profile of a heat-induced
523 *Hsph1* gene in the non-heat-shock condition (NHS), upon a 1-h heat shock (HS), and upon recovery

524 from a 1-h heat shock (Rec). Inset depicts promoter-proximal region. The dashed line indicates the
525 highest Pol II pausing density in non-heat-shocked cells and asterisks denote prominent Pol II
526 pausing on sense (orange) and anti-sense (black) strand after recovery. **C)** Average promoter-
527 proximal pausing measured at all transcribed genes. Shaded area: 12.5-87.5% confidence interval.
528 The y-axis in B is in linear scale from 172 to -172 for each track.
529
530 **Figure 2. A single heat shock primes accelerated gene induction over mitotic divisions. A)**
531 Experimental setup for measuring transcription kinetics in MEFs. Transcription was analyzed upon
532 heat shock in unconditioned cells (unCond, upper panel), and in cells that were preconditioned with
533 a 1-h heat shock and 48-h recovery (preCond, lower panel). **B)** Nascent transcription at *Ubc* in
534 unconditioned and preconditioned cells. Insets show Pol II density in promoter-proximal region in
535 unconditioned (upper panels) and preconditioned (lower panels) cells. **C)** Average intensity of
536 promoter-proximally engaged Pol II upon a 12.5-min heat shock at genes that gain a faster heat-
537 induction by preconditioning (upper panel) or at genes that are highly heat-induced regardless of
538 preconditioning (lower panels). Pol II density after the pause-release is indicated with an
539 arrowhead. Shaded area: 12.5-87.5% confidence interval. **D)** Heat-induced wave of transcription
540 along *Vcl* gene. The blue dashed region indicates an advancing wave of transcription that has
541 proceeded farther in preconditioned than in unconditioned cells upon a 12.5-min heat shock. Insets
542 show promoter-proximal Pol II density in unconditioned (upper panels) and preconditioned (lower
543 panels) cells. Grey vertical lines in insets mark 100 nt intervals.
544
545 **Figure 3. Repeated heat shocks refine basal and inducible transcription in daughter cells. A)**
546 Experimental setup for preconditioning human K562 cells with multiple heat shocks. Nascent
547 transcription was measured upon heat shock in unconditioned cells (unCond, left panel), and in
548 cells that were pre-exposed to nine 1-h heat shocks during three consecutive days and allowed to
549 recover for 48 h prior to an additional 1-h heat shock (preCond, right panel). **B)** Differential gene
550 and enhancer transcription. Up and Down denote numbers of genes (upper panels) and enhancers
551 (lower panels) with significantly heat-induced or heat-repressed Pol II density, as measured against
552 non-stressed cells (unCond 0'). **C)** Transcriptional profiles of genes with unchanged (left panel),
553 decreased (middle panel) or increased (right panel) basal transcription due to preconditioning. **D)**
554 Transcriptional profiles of genes that had lost (left panel), gained (middle panel), or accelerated
555 (right panel) heat-induction as a result of preconditioning. **E)** Average Pol II density at promoter-
556 proximal regions of heat-induced genes. Shaded area: 12.5-87.5% confidence interval.

557

558 **Figure 4. Initiation is reduced and termination prolonged in the daughters of repeatedly**
559 **stressed K562 cells. A)** Nascent transcription along *HSPH1* showing reduced density of engaged
560 Pol II at the promoter-proximal region (light blue dashed circle) and increased density downstream
561 of the Cleavage and Polyadenylation Site (CPS; green dashed circle) in preconditioned cells. **B)**
562 Promoter-proximal region of *HSPH1* showing active sites of transcription (3'-end of each PRO-
563 seq read), and initiation intensity (5'-end of each PRO-seq read). Arrowheads compare the intensity
564 of initiation, the arrow denotes transcription initiation site upon heat shock. **C)** Transcriptional
565 activity of heat-induced genes (n=587) compared with the change in Pol II density at promoter-
566 proximal region (0 to +1000 from TSS, upper panel) or termination window (+100 to +6000 from
567 CPS, lower panel) due to preconditioning. Spearman's rank correlations (rho) and the most affected
568 genes are indicated. **D)** Average density of engaged transcription complexes along highly heat-
569 induced genes in unconditioned (upper panels) and preconditioned (lower panels) cells. Light blue
570 arrowheads indicate the promoter-proximal Pol II, green arrowheads show the site of increased Pol
571 II engagement in preconditioned cells. **E)** Average ATAC-seq density at highly heat-induced genes
572 in unconditioned (upper panels) and preconditioned (lower panels) cells. Shaded area: 12.5-87.5%
573 confidence interval.

574

575 **Figure 5. HSF1 *trans*-activates genes *via* promoters and enhancers. A)** HSF1-binding intensity
576 to the *HSPH1* promoter (uppermost panel), nascent transcription of *HSPH1* as measured from the
577 first intron (middle panel), and relative level of polyA-containing *HSPH1* mRNA (bottom panel)
578 in unconditioned and preconditioned K562 cells. ** p-value <0.05; *** p-value <0.005. **B)** HSF1
579 protein expression in scrambled-transfected (Scr) and HSF1-depleted (shHSF1) K562 cells. **C)**
580 Transcription of *TAX1BP1* and its upstream enhancer in the presence and absence of HSF1. **D)**
581 Inset of *TAX1BP1* enhancer (green bar) and TSS (purple arrow), showing heat-induced HSF1
582 binding (gray) to the enhancer and TBP binding to the promoter (purple). **E)** Inset showing
583 enhancer transcription in the presence and absence of HSF1. **F)** Average Pol II density at HSF1-
584 dependently heat-induced enhancers. **G)** Average ATAC-seq density at HSF1-dependent and
585 highly transcribed enhancers. In F and G, the shaded area: 12.5-87.5% confidence interval.

586

587 **Figure 6. Prolonged termination co-occurs with decreased RNA-cleavage, and reduced**
588 **initiation at the gene's promoter and connected enhancers. A)** Schematic: 3'-nts of PRO-seq
589 reads report the active sites of transcription and 5'-nts provide a read-out for initiation (promoter-

590 proximal region) and transcript cleavage (termination window). Pol II is depicted as a red rocket
591 going from right to left. Green sphere in the end of the RNA molecule indicates 5'-cap that protects
592 the transcript from exonucleosomal degradation. **B)** Active sites of transcription at *DNAJB1* gene.
593 The boxed areas compare heat-induced transcription in unconditioned and repeatedly
594 preconditioned K562 cells. **C)** 5'-nts of PRO-seq reads along *DNAJB1*. Initiation is indicated with
595 light blue arrowheads, transcript cleavage sites are denoted with dashed red circles. **D)** Upper left
596 panel: schematic presentation of TSS-overlapping PRO-seq reads. Paused Pol II associates with
597 25-60 nt long reads, while productively elongating Pol II has proceeded beyond the +60 nt from
598 TSS. Lower left panel: lengths of TSS-overlapping PRO-seq reads at genes where Pol II
599 progression changes due to preconditioning (n=429). Upper right panel: schematic representation
600 of CPS-overlapping PRO-seq reads. Reads shorter than the maximum read length (75 nt) report
601 events of transcript cleavage. Lower right panel: lengths of CPS-spanning reads at genes with
602 changed Pol II progression (n=429). Accumulated Pol II molecules in termination windows of
603 repeatedly preconditioned cells associate with uncleaved transcripts. **E)** Fold change of engaged
604 Pol II in preconditioned over unconditioned cells at termination windows, promoter-proximal
605 regions, and connected enhancers. The red dashed line indicates fold change 1. Increased and
606 decreased denote higher and lower Pol II density after preconditioning.
607
608 **Figure 7. Model for heat-induced transcriptional memory accelerating promoter-proximal**
609 **pause-release and decelerating termination over cell divisions.** In unconditioned cells (upper
610 panel), paused Pol II is rapidly released from the promoters of heat-induced genes into elongation,
611 and it efficiently proceeds through the gene. A single heat shock exposure (lower left panel) primes
612 an additional set of genes for instant heat-induction in the daughter cells by increasing Pol II
613 pausing. Multiple heat shocks (lower right panel) cause reduced transcript cleavage at the 3'-end
614 of active genes, which decelerates termination and decreases recycling of the transcription
615 machinery to heat-activated genes and enhancers.
616
617
618 **Supplemental Figure Legends**
619
620 **Supplemental Figure 1 (related to Figures 1 and 2). Normalization of PRO-seq data for**
621 **accurate quantification of transcriptional responses in MEFs. A-B)** Correlation plots of gene
622 body transcription (log2RPK) between biological PRO-seq replicates of acute stress and recovery

623 from stress **(A)**, and rapid stress-induced transcriptional changes in unconditioned and singly
624 preconditioned MEFs **(B).** Please see Figure 2A for a schematic presentation of preconditioning
625 with a single heat shock exposure. **C)** Average profile of nascent transcription at heat-unresponsive
626 genes in unconditioned and preconditioned MEFs after normalizing the datasets against whole
627 genome run-on RNAs from spiked-in, permeabilized *Drosophila* S2 cells. **D)** Upper panel:
628 Correlation of gene body transcription (log2RPK) between non-heat-shocked cells (0') and cells
629 exposed to a 1-h heat shock followed by a 48-h recovery (1h HS + 48h Rec). Lower panel:
630 Correlation plots of gene body transcription (log2RPK) between non-heat-shocked MEFs mapped
631 in this study (y-axis) and in our previous study (x-axis; Mahat *et al*., 2016). In panels C, F-H, Rho
632 indicates Spearman rank correlation.

633

634 **Supplemental Figure 2 (related to Figure 3). Normalization of PRO-seq data for accurate**
635 **quantification of transcriptional responses in human K562 cells. A)** Correlation plots of gene
636 body transcription (log2RPK) between biological PRO-seq replicates in unconditioned and singly
637 preconditioned K562 cells. The preconditioning was conducted as for MEFs, illustrated in Figure
638 2A. **B)** Average profile of nascent transcription at heat-unresponsive genes in unconditioned and
639 singly preconditioned K562 cells after normalizing the datasets against whole genome run-on
640 RNAs from spiked-in *Drosophila* S2 cells. TSS: transcription start site; CPS: cleavage and
641 polyadenylation site.

642

643 **Supplemental Figure 3 (related to Figures 1, 3, 5 and 6). *De novo* identification of putative**
644 **enhancers by their profile of divergent transcription captures functionally verified**
645 **enhancers. A)** MYC locus in human K562 cells showing functionally verified enhancers (Fulco *et*
646 *al*., 2016) with green bars, and their physical connections to the MYC promoter, indicated by Pol
647 II ChIA-PET data. Please note that only the connections between functionally verified enhancers
648 and the MYC promoter are shown. *De novo* identified putative enhancers are indicated with blue
649 bars. The browser tracks depict GATA1 binding (Consortium EP, 2011), and nascent transcription
650 at the locus, demonstrating divergent transcription at each functionally identified enhancer. **B)** Beta
651 globin locus containing Haemoglobin subunit epsilon 1 (*HBE1*) gene and the locus control element
652 with functionally verified enhancers. The four enhancers active in erythrocyte lineages

653 (hypersensitive sites, HSSs, 1-4) are indicated with gold bars, and are shown to harbor prominent
654 GATA1 binding and divergent transcription. **C)** Average profiles of indicated chromatin marks
655 (Consortium EP, 2011) at the *de novo* identified putative enhancers. **D)** Percent of the *de novo*
656 identified enhancers that localize to transcription-linked chromatin loops, deduced from the Pol II
657 ChIA-PET data (ENCODE, GSM970213).

658

659 **Supplemental Figure 4 (related to Figures 1 and 2). Promoter-proximal Pol II pausing**
660 **changes during recovery from an acute heat shock in MEFs. A)** FACS-defined fraction of
661 mouse embryonic fibroblasts (MEFs) with indicated DNA content during heat shock, recovery,
662 and an additional heat shock exposure. Cells with a diploid genome are indicated with G1 and
663 duplicated (tetraploid) genome with G2/M. Apoptotic refers to cells with fragmented genome (sub
664 G1). **B)** Protein levels of Pol II during heat shock in unconditioned and singly preconditioned
665 MEFs. Beta-tubulin serves as a loading control. **C-D)** Transcriptional profile of a heat-repressed
666 (C) and a heat-induced (D) gene, at which promoter-proximal Pol II pausing increases (D) or
667 remains elevated (E) during recovery from a single heat shock. The lower panels show insets of
668 the promoter-proximal region, depicting the highly reproducible change in transcriptionally
669 engaged Pol II upon heat shock and recovery between the replicates.
670

671 **Supplemental Figure 5 (related to Figure 2). A subset of genes gains faster heat-**
672 **responsiveness by single preconditioning in MEFs. A)** DESeq2-analysis of differential gene
673 transcription between unconditioned (unCond) and singly preconditioned (preCond) MEFs at the
674 indicated time points of heat stress. Pol II density was quantified from gene bodies (+500 from TSS
675 to -500 from CPS). Up denotes gene bodies with significant ($p < 0.001$) increase in heat-induced
676 transcription in preconditioned cells as compared to unconditioned cells. Down denotes gene
677 bodies where transcription in preconditioned cells is significantly ($p < 0.001$) lower than in
678 unconditioned cells. In the 12.5-min time point, HS-induced indicates heat-induced genes that gain
679 higher gene body transcription, and HS-repressed denotes heat-repressed genes that gain deeper
680 transcription reduction, due to preconditioning. We refer to these genes as faster heat-induced and
681 faster heat-repressed, respectively, throughout the manuscript. **B-C)** Browser shot examples of
682 genes with faster (left panel) and slower (right panel) heat induction after preconditioning. Gene
683 body RPK (gbRPK) is indicated and bolded in 12.5-min conditions that show statistically

684 significant change between unconditioned and preconditioned cells. **D)** Average Pol II density at
685 the promoter-proximal regions of genes that are called heat-induced upon the 12.5-min time point
686 in unconditioned cells. The Pol II density in D is compared between unconditioned (black dotted
687 line) and preconditioned (yellow solid line) cells upon a 12.5-min heat shock. Arrowheads denote
688 the signal downstream of Pol II pausing, as in Figure 2C. The right panel in D depicts the region
689 around the pause in an expanded scale. Shaded area indicates 12.5-87.5% confidence interval in
690 each 20-nt window. **E)** Enriched gene ontology terms among genes that gain faster heat-induction
691 by preconditioning, are highly heat-induced regardless of preconditioning, or that are instantly
692 induced in unconditioned cells.
693
694 **Supplemental Figure 6 (related to Figures 2 and 3.) Human K562 cells precisely restore**
695 **transcription of genes and enhancers after a single heat shock. A)** DESeq2-analysis of
696 differential gene (upper panels) and enhancer (lower panels) transcription in unconditioned
697 (unCond) human K562 cells upon an acute heat shock response. Up and Down denote a statistically
698 significant increase or decrease, respectively, in Pol II density upon heat shock, as compared to
699 optimal growth conditions. Pol II density was quantified from gene bodies (+500 from TSS to -500
700 from CPS), or along the length of each enhancer. **B)** DESeq2-analysis of differential gene (left
701 panel) and enhancer (right panel) transcription 48 h after a single 1-h heat shock exposure. **C)**
702 DESeq2-analysis of differential gene (upper panels) and enhancer (lower panels) transcription
703 upon heat shock that was induced 48-h after recovery from a single 1-h heat shock (single
704 preCond).
705
706 **Supplemental Figure 7 (related to Figures 2 and 3). Human K562 cells provoke a highly**
707 **similar heat shock response in unconditioned cells and in daughters of cells that experienced**
708 **a single 1-hour heat shock. A)** DESeq2-analysis of differential gene transcription between
709 unconditioned (unCond) and singly preconditioned (preCond) K562 cells, as measured at the
710 indicated time points of heat stress. The preconditioning was conducted as for MEFs, illustrated in
711 Figure 2A. Up denotes gene bodies with significant ($p < 0.05$) increase in heat-induced transcription
712 in preconditioned cells as compared to unconditioned cells. Down denotes gene bodies where
713 transcription in preconditioned cells is significantly ($p < 0.05$) lower than in unconditioned cells.
714 **B-C)** Browser shot examples of nascent transcription at heat-induced *BAG3* **(B)** and *HSPH1* **(C)**
715 genes comparing the close to identical heat shock responses between unconditioned (unCond) and

716 preconditioned (preCond) human K562 cells. Insets depict the region around the promoter-
717 proximal pause in an expanded scale.
718
719 **Supplemental Figure 8 (related to Figure 3). Human K562 cells proliferate through repeated**
720 **heat shock exposures. A)** Relative number of K562 cells in scrambled transfected (Scr) and HSF1-
721 depleted (shHSF1) cells, as counted by dividing the number of cells at each day with the number
722 of cells at day 1. The relative cell count is plotted in a logarithmic scale, and theoretical exponential
723 growth indicated with a dotted gray line, demonstrating that K562 cells maintain their proliferation
724 rate throughout the preconditioning with nine heat shock exposures. **B)** FACS-defined fraction of
725 cells with fragmented (indicative of apoptosis), or polyploid, genome. The slightly higher number
726 of apoptotic cells in day 1 is likely a consequence of electroporation 24 h before the first heat shock
727 treatment of preconditioning. **C)** Average Pol II density along the coding and non-coding strands
728 of heat-unresponsive genes, shown in unconditioned and repeatedly preconditioned cells after
729 normalizing the samples against whole-genome spike-in from *Drosophila* S2 cells. Please note that
730 the whole-genome (isolated nuclei) spike-in allows accurate normalization between the samples
731 that were grown several days in distinct cell cultures. **D)** Correlation plots of gene body
732 transcription (log2RPK) between biological PRO-seq replicates in unconditioned (upper panels)
733 and repeatedly preconditioned (lower panels) cells. Rho indicates Spearman rank correlation. **E)**
734 Pol II protein levels during heat shock in unconditioned and repeatedly preconditioned (preCond)
735 K562 cells.
736
737 **Supplemental Figure 9 (related to Figures 2 and 3). Human K562 cells retain cell type-specific**
738 **transcription throughout repeated heat exposures, but reduce transcription of ER-linked**
739 **genes. A)** Browser track examples of basal transcription at lineage specific factor genes *TAL1*,
740 *GATA1* and *GATA2*. The distribution of nascent transcription complexes at each gene is depicted
741 in cells that were not exposed to stress (unCond), or that had recovered 48 h from nine 1-h heat
742 shocks (preCond). **B)** Browser track examples of basal transcription at genes involved in protein
743 maturation *via* endoplasmic reticulum (ER) to Golgi pathway. **C)** Enriched gene ontology terms
744 among genes that show decreased basal transcription in preconditioned cells. **D)** Basal and heat-
745 responsive transcription at cell cycle regulators *CDK1* and *CCND1* in unconditioned and
746 preconditioned K562 cells. Heat-induced run-through transcription (also known as Downstream of
747 Genes, DoG) is indicated downstream of CPS in *CDK1*.
748

749 **Supplemental Figure S10 (related to Figures 4-5). ATAC-seq data in unconditioned, singly**
750 **preconditioned, and repeatedly preconditioned K562 cells. A-B)** Correlation plots of ATAC-
751 seq replicates in unconditioned and singly preconditioned **(A)**, as well as in unconditioned and
752 repeatedly preconditioned **(B)** K562 cells. The ATAC-seq read counts were measured at each peak
753 called with MACS2 from combined bam files of all samples and replicates reported in A, respective
754 B. Rho indicates spearman rank correlation.
755
756 **Supplemental Figure S11 (related to Figure 4-5). Heat-induced gene activation triggers**
757 **increased chromatin accessibility along the gene. A)** Schematic presentation of transposase Tn5-
758 released chromatin fragments. The ends of fragments are used as indication of accessible sites,
759 whereas the middle of the fragment approximates the genomic sites that were shielded from
760 fragmentation. **B)** ATAC-seq (fragment center) and PRO-seq signal at *HSPH1* gene upon heat-
761 induced transcriptional activation in unconditioned and repeatedly preconditioned K562 cells. **(C)**
762 Insets of termination window (left panel) and promoter-proximal region (right panel) of *HSPH1.*
763 The browser tracks in insets overlay ATAC-seq signal from unconditioned (black) and repeatedly
764 preconditioned (colored) cells.
765
766 **Supplemental Figure S12 (related to Figures 4-6). Rapid nucleosomal loss at heat-induced**
767 **genes occurs in unconditioned and repeatedly preconditioned K562 cells. A)** Average ATAC-
768 seq density from whole fragments at highly heat-induced genes in unconditioned (upper panels)
769 and singly preconditioned (lower panels) cells**. B)** PRO-seq profile of active sites of transcription
770 at heat-induced *DNAJB1* gene showing similar Pol II density in singly preconditioned and
771 unconditioned K562 cells. **C-D)** Browser images of ATAC-seq signal (whole fragments) at
772 *DNAJB1*. In C, chromatin openness is compared between unconditioned (black) and singly
773 preconditioned (aqua) cells, in D, between unconditioned (black) and repeatedly preconditioned
774 (aqua) cells. The transcription profile for *DNAJB1* in repeatedly preconditioned cells is shown in
775 Figure 6B. **E-F)** MNase-coupled ChIP-qPCR measured levels of histones H2A.Z, H3 and H4, and
776 acetylation of H4 (H4ac) at the *HSPA1A* and *HSPH1* promoters and +1 nucleosomes in
777 unconditioned and repeatedly preconditioned K562 cells.
778
779 **Supplemental Figure S13 (related to Figure 5). HSF1 is indispensable for heat-induced**
780 **activation of genes and enhancers. A)** Nascent transcription profile of *HSF1* gene in
781 unconditioned and repeatedly preconditioned K562 cells. **B)** Relative levels of HSF1 mRNA in

782 unconditioned and repeatedly preconditioned K562 cells. **C)** Levels of HSF1 protein in
783 unconditioned and repeatedly preconditioned K562 cells. Beta-tubulin serves as a loading control.
784 **D)** HSF1 binding at the promoter (uppermost panel), transcription of coding sequence (middle
785 panel), and relative expression of polyA-containing mRNA (lowest panel) of *HSPA1A* in
786 unconditioned and repeatedly preconditioned K562 cells. ** indicates p-value <0.05 and *** p-
787 value <0.005. **E)** Transcription profile of HSF1-dependently heat-induced *BAG3* gene in
788 unconditioned and repeatedly preconditioned cells in the presence or absence of HSF1. **F)** HSF1-
789 dependent heat-inducibility of genes (upper panel) and enhancers (lower panel). HSF1-dependency
790 for each individual gene or enhancer was measured by dividing transcription (gene body RPK) in
791 shHSF1 by transcription in Scr, after basal transcription was removed from the level of
792 transcription upon heat shock.
793
794 **Supplemental Figure S14 (related to Figure 5). Heat-induced changes in chromatin**
795 **accessibility are highly similar in unconditioned and singly preconditioned K562 cells.** ATAC-
796 seq signal (whole fragment) at indicated enhancers in unconditioned and singly preconditioned
797 K562 cells. In A and C, the shaded area indicates 12.5-87.5% confidence interval in each 20-nt
798 window. Please note the intact heat-induced enhancer accessibility in singly preconditioned cells,
799 as comparison to the lack of chromatin opening in repeatedly stressed cells showing in Figure 5G.
800
801 **Supplemental Figure S15 (related to Figures 5 and 6). Daughters of repeatedly**
802 **preconditioned cells display a genome-wide change in Pol II distribution. A)** Schematic
803 representation of genomic regions within which the distribution of engaged Pol II molecules was
804 measured. The numbers below each region indicate the percentage of all uniquely mapping PRO-
805 seq reads that localize to the given region in unconditioned K562 cells. NHS: non-heat shock; 30
806 min and 60 min indicate the time of heat shock at 42°C. **B)** Percentage of all uniquely mapping
807 PRO-seq reads at the indicated regions of heat-induced (left panel) and heat-repressed (right panel)
808 genes and enhancers. Black dashed circles indicate genomic regions with increased total
809 engagement of Pol II in repeatedly preconditioned cells. Gray dashed circles indicate regions with
810 reduced Pol II engagement in repeatedly preconditioned cells. The colored triangles above the bars
811 denote the time of the heat shock. **C)** Heat-repressed *beta-actin* (*ACTB*) exemplifies reduced Pol
812 II engagement at the 5' region (dashed circles), and increased engagement downstream of the CPS
813 (dashed squares) in repeatedly preconditioned *versus* unconditioned cells upon heat shock. Despite
814 prominent heat-repression, the gene body transcription of *ACTB* (log2RPK in blue) remains high

815 (8.06) upon heat shock. Please see Figures 5A, 5B and 6B for examples of heat-induced genes with
816 similarly changed pattern of nascent transcription complexes in repeatedly preconditioned *versus*
817 unconditioned cells. **D)** Difference in heat-induced Pol II density between repeatedly
818 preconditioned and unconditioned K562 cells, as measured along genes that show reduced Pol II
819 engagement at the 5'-end and increased engagement downstream of CPS (n=429 genes). **E)** Gene
820 body transcription (log2RPK) plotted cumulatively for genes with unchanged (shades of gray) or
821 changed (shades of orange) distribution of Pol II due to preconditioning. Genes with changed Pol
822 II distribution constitute primarily of highly transcribed genes (median log2RPK: 6.06), whereas
823 genes with no detectable change (shades of gray) show modest transcription level (median
824 log2RPK: 3.29). **F)** Gene-by-gene comparison of the change in Pol II engagement (preCond 60' -
825 unCond 60') along the termination window (+100 to +6000 from CPS) and the promoter-proximal
826 region (0 to +1000 from TSS). Each dot is a gene with a changed Pol II distribution at '5 and 3'
827 ends (n=429). *p:* Pearson, rho: Spearman correlation. P-values for *p* and rho $<2.2x10^{-16}$. Dashed red
828 line: y = -x. **G)** Pol II density at enhancers that connect to promoters of the indicated gene groups.
829 The Pol II density at enhancers is compared between unconditioned (unCond) and repeatedly
830 preconditioned (preCond) cells upon a 60-min heat shock (HS60). Please note that only enhancers
831 that connect to genes with reduced promoter-proximal Pol II density show a simultaneous reduction
832 of Pol II counts at the enhancers. P-values are independent two-sample t-tests of the enhancer Pol
833 II densities between unconditioned and preconditioned cells.
834
835 **Supplemental Figure S16 (related to Figure 2 and Supplemental Figure 5). Flow chart**
836 **showing identification of genes with faster heat-induction or slower heat-repression in**
837 **preconditioned MEFs. Heat shock *versus* non heat shock:** Genes with significantly higher (heat-
838 induced) or lower (heat-repressed) nascent transcription were identified upon 15-min, 25-min and
839 40-min heat shock, as compared to non-stressed cells. Genes that were called significantly heat-
840 induced in any of the time points were counted in the 'all heat-induces genes' category. Genes with
841 significantly reduced transcription in any of the time points were counted in the 'all heat-repressed
842 genes' category. **Preconditioned *versus* unconditioned:** Nascent transcription in preconditioned
843 cells was compared to nascent transcription in unconditioned cells in all the heat shock time points.
844 Genes that showed higher transcription in preconditioned cells upon a 15-min heat shock (precond
845 15'/uncond 15') were intersected with all heat-induced genes. The intersection of 462 genes was
846 counted as genes with accelerated heat induction in preconditioned cells. To identity genes with
847 slower heat repression in preconditioned cells, the heat-repressed genes were intersected with genes

848 that showed lower transcription in preconditioned than in unconditioned cells upon a 15-min heat
849 shock (precond 15'/uncond 15'). The intersection of 298 genes was counted as genes with slower
850 heat-repression in preconditioned cells. In all DESeq2 analyses: p-value <0.001, and fold change
851 >1.25 (induced) or <0.8 (repressed).

852 **STAR METHODS**

853

854 **Resource Availability**

855 *Lead Contact*

856 Further information and requests for resources and reagents should be directed and will be fulfilled
857 by the Lead Contact, Prof. Lea Sistonen (lea.sistonen@abo.fi).

858

859 *Materials Availability*

860 This study did not generate new unique reagents.

861

862 *Data and Code Availability*

863 The PRO-seq and ATAC-seq datasets generated in this study have been deposited to Gene
864 Expression Omnibus (https://www.ncbi.nlm.nih.gov/geo/), and are available as raw and processed
865 files through accession numbers GSE127844, GSE154746, GSE128160 and GSE154744.
866 Original figures for Western Blotting images presented in this paper are available in Mendeley
867 (doi: 10.17632/gycj6tnw6v.1).

868

869 **Experimental Model and Subject Details**

870 In this study, human K562 erythroleukemia cells and mouse embryonic fibroblasts (MEFs) we
871 used. The K562 cell line originated from ATCC. The immortalized MEFs originate from wildtype
872 mouse (McMillan *et al*., 1998), and were obtained from Ivor Benjamin laboratory.

873

874 **Method Details**

875 *Cell Culture, Heat Treatments and Cell Cycle Profiling*

876 Cells were maintained at 37°C in a humidified 5% CO_2 atmosphere. MEFs (McMillan *et al*., 1998)
877 were cultured in Dulbecco's modified medium (Gibco), and K562 cells in RPMI (Sigma),
878 supplemented with 10% FCS, 2 mM L-glutamate, and streptomycin/penicillin (Mahat and Lis,
879 2017; Vihervaara *et al*., 2017). The 30-min and 60-min heat shock treatments were conducted by
880 submerging the cell culture into a 42°C water bath (Vihervaara *et al*., 2017). The 12.5-min, 25-
881 min, and 40-min heat shock treatments were instantly provoked by replacing the 37°C media with
882 pre-warmed pre-conditioned media (Mahat and Lis 2017). In adherent MEFs, inducing or
883 terminating heat shock does not require pelleting the cells. In K562 suspension cells, the 37°C
884 media was removed after centrifugation (1000 rpm, 4 min), and the heat shock initiated by re-

885 suspending the cells in pre-warmed (42°C) pre-conditioned media. The heat shock in K562 cells
886 was terminated by placing the 10 ml of heat shock cell suspension into 35 ml of ice-cold PBS,
887 followed by centrifugation (1000 rpm, 4 min) at 4°C. The non-heat-shocked control cells were
888 retained in similar confluence, and subjected to same treatments, but only exposed to media and
889 conditions at 37°C. Recovery from the heat shock(s) was conducted by placing the cells at 37°C in
890 a humidified 5% CO_2 atmosphere. DNA content of the cells was determined by propidium iodide
891 (PI) staining (40 µg/ml; Sigma), and progression of the cell cycle monitored by fluorescence-
892 mediated counting (FACSCalibur, BD Biosciences). The FACS histograms were generated using
893 Cell Quest Pro-6.0 (BD Biosciences) and Flowing Software 2.5 (Turku Bioscience Centre). The
894 error bars in statistical analyses indicate standard deviations.
895
896 *Depletion of HSF1 with Short Hairpin RNA*
897 HSF1 was depleted from K562 cells as previously described (Östling *et al*., 2007; Vihervaara *et*
898 *al*., 2013) using shRNA constructs ligated into pSUPER vectors (Oligoengine). The vector-
899 encoded oligonucleotides recognized HSF1 mRNA (GCT CAT TCA GTT CCT GAT C), or
900 contained a scrambled sequence (GCG CGC TTT GTA GGA TTC G) that is not predicted to bind
901 any sequence encoded by the human genome. The shRNA constructs were transfected into cells
902 by electroporation (970 µF, 220 mV) 24 h prior to the first heat treatment.
903
904 *MNase-coupled quantitative ChIP*
905 ChIP was performed as previously described (Östling *et al*., 2007; Vihervaara *et al*., 2013), with
906 the following modifications to digest the unshielded chromatin with endo- and exonuclease MNase
907 (Skene and Henikoff, 2015). After cross-linking protein-DNA interactions with 1% formaldehyde
908 for 5 min on ice, the samples were quenched with 0.125 M glycine and washed with PBS. The
909 pellets were resuspended in TM2 buffer (10 mM Tris, pH 7.5, 2 mM $MgCl_2$, 1x proteinase
910 inhibitors cocktail from Roche, 1 mM DTT), and supplemented with 1.5% NP-40 to permeabilize
911 the cells. The chromatin was fragmented using 6.3 U/µl MNase (New England Biolabs, NEB) for
912 10 min at 37°C in MNase buffer (10 mM Tris, pH 7.5, 2 mM $MgCl_2$, 2 mM $CaCl_2$, 1x proteinase
913 inhibitors cocktail from Roche, 1 mM DTT). The reaction was terminated in final concentration of
914 1% SDS and 10 mM EGTA. The digested chromatin was diluted in ChIP buffer (150 mM NaCl,
915 20 mM Tris-HCl pH 8.0, 1% Triton-X, 1x protease inhibitors from Roche), and pre-cleared with
916 uncoupled protein G coated sepharose beads (GE Heathcare). Immunoprecipitation was carried
917 over night at 4°C using the following ChIP-verified antibodies: HSF1 (Spa-901, Enzo), H2.AZ

918 (Abcam, ab4174), H3 (Merck Millipore, 06-755), H4 (Merck Millipore, 05-858) and AcH4 (06-
919 866, Upstate). Proteins were degraded with proteinase K (Thermo Fisher) and RNA with RNase A
920 (Invitrogen), and the cross-links reversed at 65°C overnight. The DNA was purified with
921 phenol:chloroform extraction and ethanol precipitation, and amplified with primers and probes
922 designed to match the exact +1 nucleosomes and promoters of *HSPA1A* and *HSPH1*. The primers
923 and probes (Table S1) were as follows. *HSPA1A* promoter: forward:
924 CTGGCCTCTGATTGGTCCAA; reverse: CACGGAGACCCGCCTTTT; probe: 5′-FAM-
925 CGGGAGGCGAAACCCCTGGAA-BHQ-3′. *HSPA1A* +1 nucleosome: forward:
926 CGGAAGGACCGAGCTCTT; reverse: GGCTCCGCTCTGAGATTG; probe: #47 (universal
927 probe library, Roche). *HSPH1* promoter: forward: GAGGCAGGTTTGAGCCAAT; reverse:
928 CGAGCCTTCTGGAAAGATTC; probe: #44 (universal probe library, Roche). *HSPH1* +1
929 nucleosome: forward: GGAAAGTTCTGATCAGTGCGATA; reverse:
930 TGAACTACCGACCCAAAAGG; probe #73 (universal probe library, Roche). The enriched
931 chromatin was quantified using TaqMan chemistry (Applied Biosystems), and the signal intensity
932 in each sample was normalized against the respective total MNase-digested DNA (input).
933
934 *Quantitative Reverse Transcription PCR*
935 For analyzing polyadenylated mRNA, RNA over 200 nt was isolated using RNeasy kit (Qiagen).
936 Subsequently, 1 µg of RNA was treated with DNase I (Promega) and reverse transcribed with
937 Moloney murine leukemia virus reverse transcriptase RNase H(–) (Promega) using oligoT primer.
938 Quantitative PCR (qPCR) reactions were run using ABI Prism 7900 (Applied Biosystems) with
939 HSPA1A, HSPH1 and GAPDH primers (Oligomer) and probes (Oligomer or Roche Applied
940 Science) reported in Table S1, and in Vihervaara *et al*. (2013) and Elsing *et al*. (2014). The forward
941 primer for HSF1 mRNA is CAAGCTGTGGACCCTCGT, the reverse
942 TCGAACACGTGGAAGCTGT, and the probe #67 (universal probe library, Roche). HSP and
943 HSF1 mRNA levels were normalized to mRNA of GAPDH, and fold inductions calculated against
944 non-treated (unCond 0') cells. All reactions were made in triplicate for samples derived from at
945 least three biological replicates. Standard deviations were calculated and are shown in the graphs.
946
947 *Western Blotting*
948 Cells were lysed in buffer C (25% glycerol, 20 mM Hepes pH 7.4, 1.5 mM $MgCl_2$, 0.42 M NaCl,
949 0.2 mM EDTA, 0.5 mM PMSF, 0.5 mM DTT), and protein concentration in the soluble fraction
950 was measured using Bradford analysis. 20 µg of total soluble protein was boiled in Laemmli sample

951 buffer, subjected to SDS-PAGE and transferred to nitrocellulose membrane (Protran nitrocellulose;
952 Schleicher & Schuell). Proteins were analyzed with primary antibodies against HSF1 (Spa-901,
953 Enzo), Pol II (Abcam, 8WG16) and β-tubulin (Abcam, ab6046). The secondary antibodies were
954 HRP conjugated (GE Healthcare), and the blots were developed using an enhanced
955 chemiluminescence method (ECL kit; GE Healthcare).
956
957 *PRO-seq*
958 PRO-seq was performed as previously described (Kwak *et al*., 2013; Mahat *et al*., 2016; Vihervaara
959 *et al*., 2017) with minor modifications. Nuclei of K562 cells were isolated in buffer A (10 mM
960 Tris-Cl pH 8.0, 300 mM sucrose, 3 mM $CaCl_2$, 2 mM $MgAc_2$, 0.1% TritonX-100, 0.5 mM DTT)
961 using Wheaton homogeniser (#357546, loose pestle). MEFs were incubated in permeabilization
962 buffer (10 mM Tris-Cl, pH 7.5, 10 mM KCl, 250 mM sucrose, 5 mM $MgCl_2$, 1 mM EGTA, 0.05%
963 Tween-20, 0.5 mM DTT, 1x protease inhibitors from Roche, 0.4 u/µl RNase inhibitor Superase In,
964 Thermo Fisher). The nuclei or permeabilized cells were flash-frozen and stored at -80°C (10 mM
965 Tris-HCl pH 8.0, 25% glycerol, 5 mM $MgAc_2$, 0.1 mM EDTA, 5 mM DTT). Before run-on
966 reaction, an equal amount of untreated *Drosophila* S2 cells was spiked into each sample, counted
967 to account for 1% of the total DNA in each run-on reaction. The following run-on reaction was
968 performed at 37°C for 3 min in the presence of biotinylated nucleotides (5 mM Tris-HCl pH 8.0,
969 150 mM KCl, 0.5% Sarkosyl, 2.5 mM $MgCl_2$, 0.5 mM DTT, 0.05 mM biotin-A/C/G/UTP from
970 Perkin Elmer, 0.4 u/µl RNase inhibitor). The total RNA was isolated with Trizol LS (Invitrogen).
971 After EtOH-precipitation, the RNA was air-dried, base hydrolyzed with 0.1 N NaOH for 5 min on
972 ice, and the NaOH was neutralized with Tris-HCl (pH 6.8). Unincorporated nucleotides were
973 removed using P-30 columns (Bio-Rad), and the biotinylated nascent transcripts were isolated in a
974 total of three rounds of streptavidin-coated magnetic bead (M-280, Invitrogen) purifications. Each
975 bead binding was followed by Trizol extraction and EtOH-precipitation of the transcripts. The 5′-
976 cap was removed with RNA 5' Pyrophosphohydrolase (Rpph, NEB), and the 5′-hydroxyl group
977 was repaired with T4 polynucleotide kinase (NEB). The libraries were generated using TruSeq
978 small-RNA adaptors and sequenced using NextSeq500 (Illumina).
979
980 *PRO-qPCR*
981 To quantify nascent RNA synthesis from selected heat-responsive genes, we modified PRO-seq to
982 perform qPCR after the 3'-adaptor ligation. In brief, run-on reactions were conducted in the
983 presence of both unlabeled (200 µM A/C/G/UTP) and biotinylated (50 µM biotin-A/C/G/UTP)

984 nucleotides during a 5-minute run-on reaction at 37°C. Total RNA isolation, base hydrolysis, and
985 3' adaptor ligation were conducted as described for PRO-seq. After the second bead binding,
986 reverse transcription was performed using a primer against the 3' adaptor, and qPCR reactions run
987 with ABI Prism 7900 (Applied Biosystems). Primers (Oligomer) and probes (Oligomer and Roche
988 Applied Sciences) were (Table S1): *HSPH1* forward: AGCAGGCGGATTGTTGTTAG; *HSPH1*
989 reverse: AAAGAGGTGGGCTAATCTTTCA; *HSPH1* probe: #38 (universal probe library,
990 Roche); *HSPA1A* forward: GCCGAGAAGGACGAGTTTGA; *HSPA1A* reverse:
991 CCTGGTACAGTCCGCTGATGA; *HSPA1A* probe: FAM-
992 TTACACACCTGCTCCAGCTCCTTCCTCTT-BHQ1; *MED26* forward:
993 ATTCCAGATGACCCGCTAAG; MED26 reverse: CGGATCACTACCACACCAGA; *MED26*
994 probe: #21 (universal probe library, Roche). The nascent transcription of *HSPA1A* and *HSPH1* was
995 compared against nascent transcription of *Mediator subunit 26* (*MED26*), a gene and a region in
996 the gene that was actively transcribed and unchanged upon heat shock (Vihervaara *et al*., 2017).
997
998 *Omni-ATAC-seq*
999 ATAC-seq was performed as previously described (Corces *et al*., 2017; Spector *et al*., 2019) using
1000 100,000 human K562 cells as starting material. Instantly after the treatments, the cells were washed
1001 with ice-cold PBS, and incubated 3 min in 100 µl ice-cold lysis buffer [10 mM Tris-Cl, pH 7.4, 10
1002 mM NaCl, 3 mM $MgCl_2$, 0.1% (vol/vol) NP-40, 1x protease inhibitor cocktail, Roche]. After
1003 centrifugation (600 g, 10 min, 4°C), the samples were re-suspended in 50 µl tagmentation buffer
1004 [10 mM Tris-Cl, pH 7.4, 10% (vol/vol) dimethyl formamide, 5 mM $MgCl_2$], and tagmentation
1005 performed with 1 µl Tn5 transposase (described in Spector *et al*., 2019) for 30 min at 37°C. DNA
1006 was isolated with phonol:chloroform extraction and ethanol precipitation using GlycoBlue
1007 (Invitrogen #AM9516) as a carrier. The correct size distribution in each library was verified by test
1008 amplifying 1/10 of the material in a dilution series, followed by visualization of the DNA in a 5%
1009 polyacrylamide gel using SYBR Gold (ThermoFisher). Half of each library was amplified 12
1010 cycles with barcoded Nextera primers (Illumina) and Q5 DNA polymerase (NEB). After
1011 amplification, the DNA fragments were size selected with Ampure XP beads (Beckman Coulter
1012 #A63880), incubating the samples first in 0.5X beads, and subsequently, in 1.8X beads. The
1013 barcoded samples were pooled, verified with Bioanalyzer, and sequenced using Illumina
1014 NexSeq500. The sequenced reads were trimmed with fastx toolkit
1015 (http://hannonlab.cshl.edu/fastx_toolkit/) and aligned to the human genome (GRCh37/hg19).
1016 Each dataset was density-normalized (fragments per million mapped fragments, FPM).

1017 Correlation of replicate pairs was assessed by first calling ATAC-seq peaks (enriched loci of
1018 chromatin accessibility) with MACS2 (Feng *et al*., 2012) using a combined bam file from all
1019 the samples in this study. Next, the count of fragments at every MACS2-called peak was
1020 measured in each sample, and replicate correlation analyzed with Spearman's rank correlation.
1021 After ensuring accurate correlation, the replicates were combined, and three types of FPM-
1022 normalized bigwig files generated, reporting the whole released fragment, the middle 20 nt of
1023 each fragment, and 10 nt at both ends of each fragment, respectively (Figure S11A). The
1024 complete raw ATAC-seq datasets (GSE154744) are available through Gene Expression
1025 Omnibus database (https://www.ncbi.nlm.nih.gov/geo/).
1026

1027 **Quantification and Statistical Analyses**

1028 *Computational Analyses of PRO-seq Data*

1029 The PRO-seq reads were adapter-clipped using cutadapt (Martin, 2011) and trimmed and filtered
1030 with fastx toolkit (http://hannonlab.cshl.edu/fastx_toolkit/). Due to usage of external spike-in
1031 material from *Drosophila* S2 cells, we combined the human (GRCh37/hg19) and *Drosophila*
1032 (dm3) genomes into a single genome file (hg19-dm3). Likewise, the mouse genome (mm10)
1033 was combined with the *Drosophila* genome (dm3) into a distinct genome file (mm10-dm3). In
1034 both cases, chromosomes of the dm3 were renamed. Reads from K562 cells were aligned to the
1035 hg19-dm3 genome and reads from MEFs to the mm10-dm3 genome, using Bowtie 2 (Langmead
1036 and Salzberg, 2012). Reads that uniquely mapped to the chromosomes of the human (hg19) or,
1037 respectively, the mouse (mm10) genome, were retained. The reads that uniquely mapped to the
1038 dm3 chromosomes provided a count of reads for spike-in derived normalization factors. The
1039 complete raw PRO-seq datasets in K562 cells (GSE127844 and GSE154746), and MEFs
1040 (GSE128160) are available through Gene Expression Omnibus database
1041 (https://www.ncbi.nlm.nih.gov/geo/).
1042

1043 *Normalization of PRO-seq Data*

1044 Mapped reads were processed from bed files to coverage files, retaining only the 3'-end
1045 nucleotide (active sites of transcription), or the 5'-end nucleotide (for analyses of initiation and
1046 cleavage), of each read. Density normalized bedgraph files were adjusted by sample-specific
1047 normalization factors that were derived either from the spike-in read count (Booth *et al*., 2018)
1048 or the count of reads at the ends (+120,000 nt from TSS to -500 nt from CPS) of long (>150 kb)
1049 genes (Mahat *et al*., 2016; Vihervaara *et al*., 2017). For samples measuring transcription during

1050 recovery from the heat shock, or the effect of multiple heat shocks, only spike-in control was
1051 utilized for normalization. When comparing transcription upon short heat shocks (12.5 min, 25
1052 min, and 40 min), we first ensured correct normalization between the unconditioned 0 min and
1053 preconditioned 0 min time points with the spike-in-derived normalization factors. Then, the 3'-
1054 ends of over 150 kb long genes were utilized to normalize samples of the rapid heat shock
1055 kinetics (unconditioned 12.5 min, 25 min and 40 min normalized against the unconditioned 0
1056 min; preconditioned 12.5 min, 25 min and 40 min against the preconditioned 0 min). This
1057 strategy allows for highly sensitive sample normalization between short heat shock time points,
1058 and usage of an extrinsic control when normalization regions within samples are not available.
1059

1060 *Quantifying Gene Transcription*

1061 Actively transcribed genes and their primarily used isoforms were identified by mapping
1062 transcription initiation sites genome-wide using discriminative regulatory elements
1063 identification from global run-on data (dREG; *https://dreg.dnasequence.org*). The most updated
1064 version of dREG (Wang *et al*., 2019) is trained to call transcription initiation sites of genes and
1065 enhancers with high sensitivity using their characteristic pattern of divergent transcription (Core
1066 *et al*., 2014; Tome *et al*., 2018). To identify gene isoforms with active transcription initiation,
1067 TSSs of RefSeq-annotated transcripts were intersected (bedtools, Quinlan and Hall, 2010) with
1068 dREG-called active regulatory elements. Subsequently, transcripts that harbored dREG-called
1069 initiation at the TSS were retained. The level of transcription *per* each annotated transcript was
1070 measured from the gene body (+500 nt from TSS to -500 nt from CPS), as described previously
1071 (Mahat *et al*., 2016; Vihervaara *et al*., 2017). In the downstream analyses, we retained a single
1072 transcript *per* gene by selecting the isoform that showed the largest fold change to heat shock,
1073 or if called unresponsive to heat stress, had the highest level of transcription in non-stress
1074 condition. The analyses of enriched gene annotation categories were performed with Database
1075 for Annotation, Visualization and Integrated Discovery (DAVID; Dennis *et al*., 2003).
1076

1077 *Identification of Transcribed Enhancers*

1078 Transcribed enhancers were identified across the genome *de novo* using dREG (Wang *et al*.,
1079 2019; *https://dreg.dnasequence.org*) that recognizes patterns of transcription at genes and
1080 enhancers. Since heat shock changes Pol II progression at regulatory elements (Vihervaara *et*
1081 *al*., 2017), we identified transcribed regulatory elements individually in each sample, and then
1082 unified the coordinates obtained from all samples using bedtools merge with d -100 (Quinlan

1083 and Hall, 2010). Subsequently, the dREG-called regulatory elements were intersected with
1084 RefSeq-annotated TSSs of genes, and only elements that did not occur at any gene promoter
1085 were retained for enhancer analyses. We confirmed that this class of distal regulatory elements
1086 robustly captured functionally verified enhancers of MYC (described by Fulco and co-workers,
1087 2016), and of LCR at the beta-globin locus (Li *et al*., 2002, Song *et al*., 2007). The occurrence
1088 of putative enhancers at sites of physical chromatin connections was investigated from existing
1089 Pol II ChIA-PET data (EGSM970213). First, the ChIA-PET-enriched sites of chromatin
1090 connections (blocks) were intersected (bedtools, Quinlan and Hall, 2010) with our putative
1091 enhancer calls, as well as with annotated TSSs of genes. Subsequently, the chromatin
1092 connections from an enhancer to an enhancer, from an enhancer to a promoter, or from an
1093 enhancer to any Pol II ChIA-PET enriched region were identified. The percentage of putative
1094 enhancers in each of these chromatin connection classes is indicated.
1095
1096 *Identifying Gene-Enhancer Loops*
1097 To annotate enhancers to their target genes, we first utilized Pol II ChIA-PET data
1098 (EGSM970213) as indicated above, identifying the set of enhancers that connected to each
1099 gene's TSS. Since chromatin capture techniques negatively select for short-range interactions,
1100 we additionally annotated enhancers within 25 kb from the gene's TSS. Pol II densities were
1101 measured at a 1,000 nt span from the dREG-called enhancer midpoint, and the average Pol II
1102 densities at connected enhancers are shown for each indicated gene group.
1103
1104 *Analyses of Differential Gene and Enhancer Transcription*
1105 To call significant changes in gene and enhancer transcription, we utilized DESeq2 (Love *et al*.,
1106 2014), which uses the variance in biological replicates to assess significant changes between
1107 conditions. Differential gene expression was quantified from gene body transcription (+500 nt
1108 from TSS to -500 nt from CPS) of each gene. In this gene body window, Pol II has passed the
1109 initiation and pause regions and is undergoing productive elongation. Enhancer transcription was
1110 quantified along the whole enhancer length, individually for minus and plus strands (Vihervaara
1111 *et al*., 2017). For significantly changed transcription, we required p-value <0.05 (K562) or
1112 <0.001 (MEFs), and fold enrichment >1.25. The less stringent criterion for K562 cells used in
1113 this study, as compared to MEFs and our earlier data on K562 cells (Vihervaara *et al*., 2017), is
1114 due to lower sequencing depth. The heat-induced changes in transcription, as well as the sets of
1115 differentially transcribed genes and enhancers are highly similar in our distinct studies of the

1116 same cell type. The identification of genes with faster heat-induction or slower heat-repression
1117 in preconditioned MEFs is depicted in Figure S16. Highly heat-induced genes displayed FC >
1118 2 in gene body transcription (heat shock / non-heat shock) and dRPK >200 (heat shock –non
1119 heat shock) at least in one of the heat shock time points as compared to non-heat shock condition.
1120

1121 *Analyses of HSF1-Dependent Transcription at Genes and Enhancers*

1122 Nascent transcription upon HSF1-knockdown was inferred from a single replicate, chosen by
1123 the most prominent down-regulation of HSF1 throughout the length of the experiment (Figure
1124 5B). To identify HSF1-dependent genes, we used two approaches. First, we measured the heat-
1125 induced gene body transcription for each gene in the presence and absence of HSF1. This
1126 comparison of transcription level identified 186 genes whose heat induction in K562 cells
1127 depleted of HSF1 remained under 50% of the respective induction in cells expressing intact
1128 levels of HSF1. Second, we used the fact that unconditioned and preconditioned cells correlated
1129 to the same extent as biological replicates (rho=0.98) and contained similar levels of gene body
1130 transcription (Figure S15B), conducting DESeq2 using the same time point from unconditioned
1131 and preconditioned cells as a replicate pair. These analyses showed 227 genes and 496 enhancers
1132 to be HSF1 dependent in both unconditioned and preconditioned K562 cells (Figure S13F). To
1133 account for a subset of genes changing basal or heat-inducible transcription due to
1134 preconditioning, we complemented the DESeq2-analysis to also find genes that showed HSF1-
1135 dependency only in unconditioned or preconditioned cells, or that were called insignificant due
1136 to changes in basal transcription. Since HSF1-dependency of the 227 DESeq2-called genes
1137 ranged from 64.1% to 99.9% (Figure S13F), we queried genes that in either unconditioned or
1138 preconditioned cells were HSF1-dependent at least to 64.1%, gained at least two-fold heat-
1139 induction, and had a minimum gene body transcription of 50 RPK in any condition. This analysis
1140 identified 18 additional HSF1-dependent genes, including *PPP1R15A* that had lost heat-
1141 inducibility, and *HSPA8* that had gained higher basal transcription, upon preconditioning. All
1142 of the 18 genes were individually verified to be HSF1-dependent by browsing.
1143

1144 *Visualizing Transcriptionally Engaged Pol II in Genome Browsers and as Composite Profiles*

1145 Pol II densities as bigWig and bedgraph files were visualized with Integrative Genomics Viewer
1146 (IGV; Thorvaldsdóttir *et al*., 2013) and an in-house browser (Hojoong Kwak, Cornell
1147 University, Ithaca, NY, USA). The scale of y-axis is equal and linear for tracks across different
1148 conditions for an indicated genomic region. To generate composite profiles, the read counts in

1149 defined genomic regions were obtained, and composite profiles generated using bigWig package
1150 (https://github.com/andrelmartins/bigWig/). The average intensities in composite profiles were
1151 queried in 20-nt, 10-nt or 1-nt bins. The shaded areas display 12.5-87.5% fractions of the data
1152 in each queried window. To generate an average profile of gene bodies with different lengths,
1153 1/500 of the gene body length was set to the bin size, after filtering out short genes where the
1154 bin would have been less than 1 nt.
1155
1156 *Identification of Genes with Compromised Pol II Progression*
1157 To identify genes with decreased Pol II density in 5'- and increased density in 3'-region, genes
1158 were first divided into three distinct regions: 1) 5'-coding region comprising 1000 nt
1159 downstream of the mid coordinate between Pol II pause sites of divergent transcription, 2) gene
1160 body, measured from +1000 nt from the mid of the pause sites to -1000 nt from the CPS, and 3)
1161 downstream, +100 nt to +6000 nt, of the CPS. PRO-seq reads in each region were measured,
1162 after which the read count in the preconditioned 60-min heat shock sample was deduced from
1163 the respective read count in the unconditioned 60-min heat shock sample. Since gene body
1164 transcription varies from gene to gene, we compared the change in Pol II progression within
1165 each gene. To identify genes with reduced 5'- and increased 3'- Pol II density, we required the
1166 reduction at 5'-coding region to be three times larger than the absolute change in the gene body
1167 read count. Simultaneously, the increase in read counts downstream of the CPS was required to
1168 be three times higher than the absolute change in the gene body read count.
1169
1170 *Quantifying Engaged Pol II Molecules in Distinct Genomic Regions*
1171 The mapped reads were sorted to distinct genomic regions by intersecting the 3'-coordinate of
1172 the read with the genomic coordinates described in Figure S15A. To avoid double mapping,
1173 gene body reads that overlapped with enhancers or pause regions were omitted. Subsequently,
1174 the number of reads in a given region was counted as fraction of total uniquely mapping reads
1175 in the PRO-seq data.
1176
1177 *Additional Datasets Used*
1178 Besides the PRO-seq (GSE127844, GSE128160 and GSE154746) and ATAC-seq (GSE154744)
1179 datasets generated in this study, the following datasets have been utilized: HSF1-binding sites
1180 in non-stressed and 30-min heat-shocked K562 cells (GSE43579; Vihervaara *et al*., 2013),
1181 binding sites of TBP (GSM935495), GATA1 (GSM935540) and GATA2 (GSM935373) in non-

1182 stressed K562 cells (Consortium EP, 2011); DNase I hypersensitive (GSM736629), MNase
1183 resistant (GSM920557), as well as H3K9me1 (GSM733777), H3K27ac (GSM733656),
1184 H3K4me1 (GSM733692) and H3K4me3 (GSM733680) enriched loci in non-stressed K562 cells
1185 (Consortium EP, 2011); Pol II ChIA-PET in non-stressed K562 cells (GSM970213); PRO-seq
1186 data in non-stressed and 30-min heat-shocked K562 cells for verification purposes (GSE89230;
1187 Vihervaara *et al*., 2017); PRO-seq data in non-stressed and 12.5-min heat-shocked MEFs
1188 (GSE71708; Mahat *et al*., 2016).
1189
1190 *Code Availability*
1191 Computational analyses have been performed using Unix, R and Python languages. Custom
1192 made scripts can be made available upon request.
1193
1194
1195 **Supplemental Material**
1196 The supplemental material contains sixteen (S1-16) figures, two tables (Supplemental Table 1 and
1197 Key Resource Table) and two datasets (Supplemental Datasets 1-2). The Supplemental Table 1
1198 contains primer and probe sequences used in this study. The Supplemental Dataset 1 lists gene
1199 transcripts in human K562 cells that show transcription initiation at the TSS, identified from PRO-
1200 seq data using dREG gateway. The Supplemental Dataset 2 lists HSF1-dependently heat-induced
1201 genes in unconditioned and preconditioned K562 cells. The abbreviations in the Supplemental
1202 Datasets are as follows. chr: chromosome. txStart: the first coordinate of the transcript (RefSeq).
1203 txEnd: the last coordinate of the transcript (RefSeq). Please note that txStart < txEnd, regardless
1204 whether the gene is on plus or minus strand. Strand: strand encoding the transcript. geneName: the
1205 name of the gene. txID: transcript specification. uC30_to_uC0: DESeq2-called regulation of
1206 transcription in unCond 30' *versus* unCond 0'. pC0_to_uC0: DESeq2-called regulation of
1207 transcription in preCond 0' *versus* unCond 0'. pC30_to_uC0: DESeq2-called regulation of
1208 transcription in preCond 30' *versus* unCond 0'. UnExp: unexpressed genes (initiation of
1209 transcription is detected, but the level of engaged Pol II molecules on the gene body is very low).
1210 UnReg: unregulated. DownHC: down-regulated with high confidence (counted as down-regulated
1211 in this study). DownLC: down-regulated with low confidence. UpHC: up-regulated with high
1212 confidence (counted as up-regulated in this study). UpLC: up-regulated with low confidence.
1213 Please note that in the manuscript, only one transcript per gene is included in the downstream
1214 analyses.

1215

1216

1217 **References**

1218

1219 Ahn, S.G., Liu, P.C., Klyachko, K., Morimoto, R.I. and Thiele, D.J. (2001). The loop domain of
1220 heat shock transcription factor 1 dictates DNA-binding specificity and responses to heat stress.
1221 Genes Dev. *15*, 2134-2145.

1222

1223 Azofeifa, J.G. and Dowell, R.D. (2017). A generative model for the behavior of RNA polymerase.
1224 Bioinformatics *33*, 227-234.

1225

1226 Boettiger, A.N. and Levine, M. (2009). Synchronous and stochastic patterns of gene activation in
1227 the Drosophila embryo. Science *325*, 471-473.

1228

1229 Booth, G.T., Parua, P.K., Sansó, M., Fisher, R.P. and Lis, J.T. (2018). Cdk9 regulates a promoter-
1230 proximal checkpoint to modulate RNA polymerase II elongation rate in fission yeast. Nat.
1231 Commun. *9*, 543.

1232

1233 Buenrostro, J.D., Giresi, P.G., Zaba, L.C., Chang, H.Y. and Greenleaf, W.J. (2013). Transposition
1234 of native chromatin for fast and sensitive epigenomic profiling of open chromatin, DNA-binding
1235 proteins and nucleosome position. Nat. Methods. *10*, 1213-1218.

1236

1237 Cardiello, J.F., Sanchez, G.J., Allen, M.A., and Dowell, R.D. (2020). Lessons from eRNAs:
1238 understanding transcriptional regulation through the lens of nascent RNAs, Transcription *11*: 3-
1239 18.

1240

1241 Chatterjee, S. and Burns, T.F. (2017). Targeting Heat Shock Proteins in Cancer: A Promising
1242 Therapeutic Approach. Int. J. Mol. Sci. *18*, E1978.

1243

1244 Chen, M. and Xie, S. (2018). Therapeutic targeting of cellular stress responses in cancer. Thorac.
1245 Cancer *9*: 1575-1582.

1246

1247 Chu, T., Rice, E.J., Booth, G.T., Salamanca, H.H., Wang, Z., Core, L.J., Longo, S.L., Corona, R.J.,
1248 Chin, L.S., Lis, J.T., Kwak, H. and Danko, C.G. (2018). Chromatin run-on and sequencing maps
1249 the transcriptional regulatory landscape of glioblastoma multiforme. Nat. Genet. *50*, 1553-1564.

1250

1251 Consortium EP, ENCODE Project Consortium. (2011). A user's guide to the encyclopedia of
1252 DNA elements (ENCODE). PLoS Biol. *9*, e1001046.

1253

1254 Core, L.J., Martins, A.L., Danko, C.G., Waters, C.T., Siepel, A. and Lis, J.T. (2014). Analysis of
1255 nascent RNA identifies a unified architecture of initiation regions at mammalian promoters and
1256 enhancers. Nat. Genet. *46*, 1311-1320.
1257
1258 Corces, M.R., Buenrostro, J.D., Wu, B. Koenig, J.L., Snyder, M.P., Pritchard, J.K., Kundaje, A.,
1259 Greenleaf, W.J. *et al.* (2016). Lineage-specific and single-cell chromatin accessibility charts
1260 human hematopoiesis and leukemia evolution. Nat. Genet. *48*: 1193-1203.
1261
1262 Dennis, G. Jr., Sherman, B.T., Hosack, D.A., Yang, J., Gao, W., Lane, H.C. and Lempicki, R.A.
1263 (2003). DAVID: Database for Annotation, Visualization, and Integrated Discovery. Genome Biol.
1264 *4*:3.
1265
1266 Duarte, F.M., Fuda, N.J., Mahat, D.B., Core, L.J., Guertin, M.J. and Lis, J.T. (2016). Transcription
1267 factors GAF and HSF act at distinct regulatory steps to modulate stress-induced gene activation.
1268 Genes Dev. *30*, 1731-1746.
1269
1270 D'Urso, A. and Brickner, J.H. (2017). Epigenetic transcriptional memory. Curr. Genet. *63*, 435-
1271 439.
1272
1273 D'Urso, A., Takahashi, Y.H., Xiong, B., Marone, J., Coukos, R., Randise-Hinchliff, C., Wang, J.P.,
1274 Shilatifard, A. and Brickner, J.H. (2016). Set1/COMPASS and Mediator are repurposed to promote
1275 epigenetic transcriptional memory. eLife *23*, 5.
1276
1277 Elsing, A.N., Aspelin, C., Björk, J.K., Bergman, H.A., Himanen, S.V., Kallio, M.J., Roos-Mattjus,
1278 P. and Sistonen, L. (2014). Expression of HSF2 decreases in mitosis to enable stress-inducible
1279 transcription and cell survival. J. Cell Biol. *206*, 735-749.
1280
1281 Feng, J., Liu, T., Qin, B., Zhang, Y. and Liu, X. S. (2012). Identifying ChIP-seq enrichment using
1282 MACS. Nat. Protoc. *7*, 1728-1740.
1283
1284 Field, A. and Adelman, K. (2020). Evaluating enhancer function and transcription. Annu. Rev.
1285 Biochem. *89*, 213-234.
1286
1287 Fujiwara, T., O'Geen, H., Keles, S., Blahnik, K., Linnemann, A.K., Kang, Y.A., Choi, K., Farnham,
1288 P.J. and Bresnick, E.H. (2009). Discovering hematopoietic mechanisms through genome-wide
1289 analysis of GATA factor chromatin occupancy. Mol. Cell *36*, 667-681.
1290
1291 Fulco, C.P., Munschauer, M., Anyoha, R., Munson, G., Grossman, S.R., Perez, E.M., Kane, M.,
1292 Cleary, B., Lander, E.S. and Engreitz, J.M. (2016). Systematic mapping of functional enhancer-
1293 promoter connections with crispr interference. Science *354*: 769-773.
1294
1295 Gerner, E.W. and Schneider, M.J. (1975). Induced thermal resistance in HeLa cells. Nature *256*,

1296 500-502.
1297
1298 Gökbuget, D. and Blelloch, R. (2019). Epigenetic control of transcriptional regulation in
1299 pluripotency and early differentiation. Development *146*, 164772.
1300
1301 Guan, Z., Giustetto, M., Lomvardas, S., Kim, J.H., Miniaci, M.C., Schwartz, J.H., Thanos, D. and
1302 Kandel, E.R. (2002). Integration of long-term-memory-related synaptic plasticity involves
1303 bidirectional regulation of gene expression and chromatin structure. Cell *111*, 483-493.
1304
1305 Guertin, M.J. and Lis, J.T. (2010). Chromatin landscape dictates HSF binding to target DNA
1306 elements. PLoS Genet. *6*, e1001114.
1307
1308 Gurdon, J.B., Elsdale, T.R., and Fischberg, M. (1958). Sexually mature individuals of Xenopus
1309 laevis from the transplantation of single somatic nuclei. Nature *182*, 64-65.
1310
1311 Hanahan, D. and Weinberg, R.A. (2011). Hallmarks of cancer: the next generation. Cell *144*, 646-
1312 674.
1313
1314 Harding, H.P., Zhang, Y., Scheuner, D., Chen, J.J., Kaufman, R.J. and Ron, D. (2009). Ppp1r15
1315 gene knockout reveals an essential role for translation initiation factor 2 alpha (eIF2alpha)
1316 dephosphorylation in mammalian development. Proc. Natl. Acad. Sci. U.S.A. *106*, 1832-1837.
1317
1318 Heard, E. and Martienssen R.A. (2014). Transgenerational epigenetic inheritance: myths and
1319 mechanisms. Cell *157*, 95-109.
1320
1321 Henriques, T., Scruggs, B.S., Inouye, M.O., Muse, G.W., Williams, L.H., Burkholder, A.B.,
1322 Lavender, C.A., Fargo, D.C. and Adelman, K. (2018). Widespread transcriptional pausing and
1323 elongation control at enhancers. Genes Dev. *32*, 26-41.
1324
1325 Huang, J., Liu, X., Li, D., Shao, Z., Cao, H., Zhang, Y., Trompouki, E., Bowman, T. V., Zon, L.
1326 I., Yuan, G. C., Orkin, S. H. and Xu, J. (2016). Dynamic control of enhancer repertoires drives
1327 lineage and stage-specific transcription during hematopoiesis. Dev. Cell *36*, 9-23.
1328
1329 Ingolia, T.D. and Craig, E.A. (1982). Drosophila gene related to the major heat shock-induced gene
1330 is transcribed at normal temperatures and not induced by heat shock. Proc. Natl. Acad. Sci. U.S.A.
1331 *79*: 525-529.
1332
1333 Kaati, G., Bygren, L.O. and Edvinsson, S. (2002). Cardiovascular and diabetes mortality
1334 determined by nutrition during parents' and grandparents' slow growth period. Eur. J. Hum. Genet.
1335 *10*, 682-688.
1336

1337 Kampinga, H.H., Hageman, J., Vos, M.J., Kubota, H., Tanguay, R.M., Bruford, E.A., Cheetham,
1338 M.E., Chen, B. and Hightower, L.E. (2009). Guidelines for the nomenclature of the human heat
1339 shock proteins. Cell Stress Chap. *14*, 105-111.
1340
1341 Klimczak, M., Biecek, P., Zylicz, A. and Zylicz, M. (2019). Heat shock proteins create a signature
1342 to predict the clinical outcome in breast cancer. Sci. Rep. *9*, 7507.
1343
1344 Koeffler, H.P. and Golde, D.W. (1980). Human myeloid leukemia cell lines: a review. Blood *56*,
1345 344-350.
1346
1347 Kwak, H., Fuda, N. J., Core, L. J. and Lis, J.T. (2013). Precise maps of RNA polymerase reveal
1348 how promoters direct initiation and pausing. Science *339*, 950-953.
1349
1350 Lämke, J., Brzezinka, K. and Bäurle I. (2016). HSFA2 orchestrates transcriptional dynamics after
1351 heat stress in Arabidopsis thaliana. Transcription *7*, 111-114.
1352
1353 Langmead, B. and Salzberg, S. (2012). Fast gapped-read alignment with Bowtie 2. Nat. Methods
1354 *9*, 357-359.
1355
1356 Leppä, S., Kajanne, R., Arminen, L. and Sistonen, L. (2001). Differential induction of Hsp70-
1357 encoding genes in human hematopoietic cells. J. Biol. Chem. *276*, 13713-31719.
1358
1359 Li, Q., Peterson, K.R., Fang, X. and Stamatoyannopoulos, G. (2002). Locus control region. Blood
1360 *100*, 3077-3086.
1361
1362 Love, M. I., Huber, W. and Anders, S. (2014). Moderated estimation of fold change and
1363 dispersion for RNA-seq data with DESeq2. Genome Biol. *15*, 550.
1364
1365 Lozzio, C.B. and Lozzio, B.B. (1975). Human chronic myelogenous leukemia cell-line with 739
1366 positive Philadelphia chromosome. Blood 45, 321-334.
1367
1368 Luft, J.C., Benjamin, I.J., Mestril, R. and Dix, D.J. (2001). Heat shock factor 1-mediated
1369 thermotolerance prevents cell death and results in G2/M cell cycle arrest. Cell Stress Chaperones
1370 *6*, 326-36.
1371
1372 Mahat, D.B. and Lis, J.T. (2017). Use of conditioned media is critical for studies of regulation in
1373 response to rapid heat shock. Cell Stress Chaperones *22*, 155-162.
1374
1375 Mahat, D.B., Salamanca, H.H., Duarte, F.M., Danko, C.G. and Lis, J.T. (2016). Mammalian heat
1376 shock response and mechanisms underlying its genome-wide transcriptional regulation. Mol. Cell
1377 *62*, 63-78.
1378

1379 Martin, M. (2011). Cutadapt removes adapter sequences from high-throughput sequencing reads.
1380 EMBnet. J. *17*, 10-12.
1381
1382 Maytin, E.V., Wimberly, J.M. and Anderson, R.R. (1990). Thermotolerance and the heat shock
1383 response in normal human keratinocytes in culture. J. Invest. Dermatol. *95*, 635-642.
1384
1385 McMillan, D.R., Xiao, X., Shao, L., Graves, K. and Benjamin, I.J. (1998). Targeted disruption of
1386 heat shock transcription factor 1 abolishes thermotolerance and protection against heat-inducible
1387 apoptosis. J. Biol. Chem. *273*, 7523-7528.
1388
1389 Melgar, M.F., Collins, F.S. and Sethupathy, P. (2011) Discovery of active enhancers through
1390 bidirectional expression of short transcripts. *Genome Biol*. **12**: R113.
1391
1392 Mikhaylichenko, O., Bondarenko, V., Harnett, D., Schor, I.E., Males, M., Viales, R.R. and Furlong,
1393 E.E.M. (2018) The degree of enhancer or promoter activity is reflected by the levels and
1394 directionality of eRNA transcription. Genes Dev. *32*, 42-57.
1395
1396 Mivechi, N.F. (1989). Heat sensitivity, thermotolerance, and profile of heat shock protein synthesis
1397 of human myelogenous leukemias. Cancer Res. *49*, 1954-1958.
1398
1399 Mueller, B., Mieczkowski, J., Kundu, S., Wang, P., Sadreyev, R., Tolstorukov, M.Y. and Kingston,
1400 R.E. (2017). Widespread changes in nucleosome accessibility without changes in nucleosome
1401 occupancy during a rapid transcriptional induction. Genes Dev. *31*, 451-462.
1402
1403 Nechaev, S., Fargo, D.C., dos Santos, G., Liu, L., Gao, Y. and Adelman K. (2010). Global analysis
1404 of short RNAs reveals widespread promoter-proximal stalling and arrest of Pol II in Drosophila.
1405 Science *327*, 335-338.
1406
1407 Niskanen, E.A., Malinen, M., Sutinen, P., Toropainen, S., Paakinaho, V., Vihervaara, A., Joutsen,
1408 J., Kaikkonen, M.U., Sistonen, L. and Palvimo, J.J. (2015). Global SUMOylation on active
1409 chromatin is an acute heat stress response restricting transcription. Genome Biol. *16*, 153.
1410
1411 Östling, P., Björk, J.K., Roos-Mattjus, P., Mezger, V. and Sistonen, L. (2007). Heat shock factor 2
1412 (HSF2) contributes to inducible expression of hsp genes through interplay with HSF1. J. Biol.
1413 Chem. *282*, 7077-7086.
1414
1415 Perez, M.F. and Lehner, B. (2019). Intergenerational and transgenerational epigenetic inheritance
1416 in animals. Nat. Cell Biol. *21*: 143-151.
1417
1418 Perino, M. and Veenstra, G.J. (2016). Chromatin control of developmental dynamics and plasticity.
1419 Dev. Cell *38*, 610-20.
1420

1421 Petesch, S.J. and Lis, J.T. (2008). Rapid, transcription-independent loss of nucleosomes over a
1422 large chromatin domain at Hsp70 loci. Cell *134*, 74-84.
1423
1424 Petesch, S.J. and Lis, J.T. (2012). Activator-induced spread of poly(ADP-ribose) polymerase
1425 promotes nucleosome loss at Hsp70. Mol. Cell *45*, 64-74.
1426
1427 Proudfoot, N. J. (2016). Transcriptional termination in mammals: Stopping the RNA polymerase
1428 II juggernaut. Science *352*, aad9926.
1429
1430 Quinlan, A.R. and Hall, I.M. (2010). BEDTools: a flexible suite of utilities for comparing
1431 genomic features. Bioinformatics *26*, 841-842.
1432
1433 Rasmussen, E.B. and Lis, J.T. (1993). In vivo transcriptional pausing and cap formation on three
1434 Drosophila heat shock genes. Proc. Natl. Acad. Sci. U. S. A. *90*, 7923-7927.
1435
1436 Ray, J., Munn, P.R., Vihervaara, A., Ozer, A., Danko, C.G. and Lis, J.T. (2019). Chromatin
1437 conformation remains stable upon extensive transcriptional changes driven by heat shock. Proc. Natl.
1438 Acad. Sci. U. S. A. 116, 19431-19439.
1439
1440 Rougvie, A.E. and Lis, J.T. (1988). The RNA polymerase II molecule at the 5' end of the uninduced
1441 hsp70 gene of D. melanogaster is transcriptionally engaged. Cell *54*, 795-804.
1442
1443 Sailaja, B.S., Cohen-Carmon, D., Zimmerman, G., Soreq, H. and Meshorer, E. (2012). Stress-
1444 induced epigenetic transcriptional memory of acetylcholinesterase by HDAC4. Proc. Natl. Acad.
1445 Sci. U.S.A. *109*, E3687-3695.
1446
1447 Skene, P.J. and Henikoff, S. (2015). A simple method for generating high-resolution maps of
1448 genome-wide protein binding. Elife *4*, e09225.
1449
1450 Song, S.H., Hou, C. and Dean, A. (2007). A positive role for NLI/Ldb1 in long-range beta-globin
1451 locus region function. Mol. Cell *28*, 810-822.
1452
1453 Spektor, R., Tippens, N.D., Mimoso, C.A. and Soloway, P.D. (2019). methyl-ATAC-seq measures
1454 DNA methylation at accessible chromatin. Genome Res. *29*: 969-977.
1455
1456 Takahashi, K. and Yamanaka, S. (2006). Induction of pluripotent stem cells from mouse embryonic
1457 and adult fibroblast cultures by defined factors. Cell *126*, 663-676.
1458
1459 Takahashi, K. and Yamanaka S. (2015). A developmental framework for induced pluripotency.
1460 Development *142*, 3274-3285.
1461

1462 Tetievsky, A. and Horowitz, M. (2010). Posttranslational modifications in histones underlie heat
1463 acclimation-mediated cytoprotective memory. J. Appl. Physiol. (1985) *109*, 1552-1561.
1464
1465 Thorvaldsdóttir, H., Robinson, J.T. and Mesirov, J.P. (2013). Integrative Genomics Viewer (IGV):
1466 high-performance genomics data visualization and exploration. Brief Bioinform. *14*, 178- 192.
1467
1468 Tippens, N.D., King, J.L., Leung, Y., Ozer, A., Booth, J.G., Lis, J.T. and Yu, H. (2020)
1469 Transcription imparts architecture, function, and logic to enhancer units. Nat. Genet. *52*, 1067-1075.
1470
1471 Tippens, N.D., Vihervaara, A. and Lis, J.T. (2018). Enhancer transcription: what, where, when,
1472 and why? Genes Dev. *32*, 1-3.
1473
1474 Tome, J.M., Tippens, N.D. and Lis, J.T. (2018). Single-molecule nascent RNA sequencing
1475 identifies regulatory domain architecture at promoters and enhancers. Nat. Genet. *50*, 1533-1541.
1476
1477 Vihervaara, A., Duarte, F.M. and Lis, J.T. (2018). Molecular mechanisms driving transcriptional
1478 stress responses. Nat. Rev. Genet. *19*, 385-397.
1479
1480 Vihervaara, A., Mahat, D.B., Guertin, M.J., Chu, T., Danko, C.G., Lis, J.T. and Sistonen, L. (2017).
1481 Transcriptional response to stress is pre-wired by promoter and enhancer architecture. Nat.
1482 Commun. *8*, 255.
1483
1484 Vihervaara, A., Sergelius, C., Vasara, J., Blom, M.A.H., Elsing. A.N., Roos-Mattjus, P. and
1485 Sistonen, L. (2013). Transcriptional response to stress in the dynamic chromatin environment of
1486 cycling and mitotic cells. Proc. Natl. Acad. Sci. U.S.A. *110*, E3388–E3397.
1487
1488 Vihervaara, A. and Sistonen, L. (2014). HSF1 at a glance. J. Cell Sci. *127*, 261-266.
1489
1490 Vilborg, A., Sabath, N., Wiesel, Y., Nathans, J., Levy-Adam, F., Yario, T.A., Steitz, J. A. and
1491 Shalgi, R. (2017). Comparative analysis reveals genomic features of stress-induced transcriptional
1492 readthrough. Proc. Natl. Acad. Sci. U.S.A. *114*: E8362-E8371.
1493
1494 Waddington, C.H. (1957). The strategy of the genes. A discussion of some aspects of theoretical
1495 biology. With an appendix by H. Kacser. London: George Allen & Unwin, Ltd.
1496
1497 Walter, P. and Ron, D. (2011). The unfolded protein response: from stress pathway to homeostatic
1498 regulation. Science *334*, 1081-1086.
1499
1500 Wang, Z., Chu, T., Choate, L.A. and Danko, C.G. (2019). Identification of regulatory elements
1501 from nascent transcription using dREG. Genome Res. *29*, 293-303.
1502

1503 Wei, Y., Schatten, H. and Sun, Q.Y. (2014). Environmental epigenetic inheritance through gametes
1504 and implications for human reproduction. Human Reproduction Update *21*, 194-208.
1505
1506 Wissink., E.M., Vihervaara, A., Tippens, N.D. and Lis, J.T. (2019). Nascent RNA analyses:
1507 tracking transcription and its regulation. Nat. Rev. Genet. *20*: 705-723.
1508
1509 Wu, W. Morrissey, C.S., Keller, C.A., Mishra, T., Pimkin, M., Blobel, G.A., Weiss, M.J. and
1510 Hardison, R.C. (2014). Dynamic shifts in occupancy by TAL1 are guided by GATA factors and
1511 drive large-scale reprogramming of gene expression during hematopoiesis. Genome Res. *24*, 1945-
1512 1962.
1513
1514 Yost, H.J. and Lindquist, S. (1991). Heat shock proteins affect RNA processing during the heat
1515 shock response of Saccharomyces cerevisiae. Mol. Cell. Biol. *11*, 1062-1068.
1516
1517 Zhang, F., Kumano, M., Beraldi, E., Fazli, L., Du, C., Moore, S., Sorensen, P., Zoubeidi, A. and
1518 Gleave, M.E. (2014). Clusterin facilitates stress-induced lipidation of LC3 and autophagosome
1519 biogenesis to enhance cancer cell survival. Nat. Commun. *5*, 5775.
1520
1521 Zobeck, K.L, Buckley, M.S, Zipfel, W.R. and Lis, J.T. (2010). Recruitment timing and dynamics
1522 of transcription factors at the Hsp70 loci in living cells. Mol. Cell *40*, 965-975.
1523